Arteriosclerosis, Thrombosis, and Vascular Biology

BASIC SCIENCES

Neutrophils Protect Against *Staphylococcus aureus* Endocarditis Progression Independent of Extracellular Trap Release

Severien Meyers, Marleen Lox, Sirima Kraisin, Laurens Liesenborghs, Caroline P. Martens, Liesbeth Frederix, Stijn Van Bruggen, Marilena Crescente, Dominique Missiakas, Pieter Baatsen, Thomas Vanassche, Peter Verhamme, Kimberly Martinod

BACKGROUND: Infective endocarditis (IE) is characterized by an infected thrombus at the heart valves. How bacteria bypass the immune system and cause these thrombi remains unclear. Neutrophils releasing NETs (neutrophil extracellular traps) lie at this interface between host defense and coagulation. We aimed to determine the role of NETs in IE immunothrombosis.

METHODS: We used a murine model of *Staphylococcus aureus* endocarditis in which IE is provoked on inflamed heart valves and characterized IE thrombus content by immunostaining identifying NETs. Antibody-mediated neutrophil depletion and neutrophil-selective PAD4 (peptidylarginine deiminase 4)-knockout mice were used to clarify the role of neutrophils and NETs, respectively. *S. aureus* mutants deficient in key virulence factors related to immunothrombosis (nucleases or staphylocoagulases) were investigated.

RESULTS: Neutrophils releasing NETs were present in infected thrombi and within cellular infiltrates in the surrounding vasculature. Neutrophil depletion increased occurrence of IE, whereas neutrophil-selective impairment of NET formation did not alter IE occurrence. Absence of *S. aureus* nuclease, which degrades NETs, did not affect endocarditis outcome. In contrast, absence of staphylocoagulases (coagulase and von Willebrand factor binding protein) led to improved survival, decreased bacteremia, smaller infiltrates, and decreased tissue destruction. Significantly more NETs were present in these vegetations, which correlated with decreased bacteria and cell death in the adjacent vascular wall.

CONCLUSIONS: Neutrophils protect against IE independent of NET release. Absence of *S. aureus* coagulases, but not nucleases, reduced IE severity and increased NET levels. Staphylocoagulase-induced fibrin likely hampers NETs from constraining infection and the resultant tissue damage, a hallmark of valve destruction in IE.

GRAPHIC ABSTRACT: A graphic abstract is available for this article.

Key Words: coagulases ■ endocarditis ■ extracellular traps ■ neutrophils ■ *Staphylococcus aureus*

Staphylococcus aureus (*S. aureus*) is the leading cause of infective endocarditis (IE), which is at its core an infected blood clot or vegetation attached to a cardiac valve, accompanied by inflammation and valve destruction.[1] Over the past 3 decades, the incidence of IE has increased, and mortality rates as high as 30% have not changed.[2–7] In contrast to endocarditis provoked by other pathogens, *S. aureus* endocarditis is associated with higher mortality and more frequent complications.[5,6,8] So far, the development of new therapies for this devastating disease has been limited, in part due to its poorly understood pathophysiology.

See cover image

Since the development of the first IE rabbit model by Ottomar Rosenbach in 1878,[9] animal models have been

Correspondence to: Kimberly Martinod, PhD, Department of Cardiovascular Sciences, KU Leuven, 49 Herestraat, Bus 911, 3000 Leuven, Belgium. Email kim.martinod@kuleuven.be

Supplemental Material is available at https://www.ahajournals.org/doi/suppl/10.1161/ATVBAHA.122.317800.
For Sources of Funding and Disclosures, see page 284.

Arterioscler Thromb Vasc Biol is available at www.ahajournals.org/journal/atvb

Nonstandard Abbreviations and Acronyms

BSA	bovine serum albumin
Coa	staphylocoagulase
H3Cit	citrullinated histone H3
IE	infective endocarditis
Ly6G	lymphocyte antigen 6 complex locus G6D
MPO	myeloperoxidase
MRP8	myeloid related protein 8
NETosis	the process of NET formation
NETs	neutrophil extracellular traps
PAD4	peptidylarginine deiminase 4
vWbp	von Willebrand factor binding protein
VWF	von Willebrand factor

Highlights

- Neutrophils and neutrophils releasing neutrophil extracellular traps are abundantly present in the surrounding vasculature of endocarditis vegetations.
- Neutrophils protect against inflammation-induced endocarditis, independent of PAD4 (peptidylarginine deiminase 4)-mediated NET (neutrophil extracellular trap) release.
- Absence of staphylocoagulases improves the outcome of infective endocarditis and diminishes infiltrate size and tissue destruction.
- Staphylocoagulases may prevent NETs from constraining infection and hampering tissue destruction.

widely used to gain insights into IE pathophysiology but have utilized approaches that mimic foreign material infection or IE associated with damaged valves[10–15] Although native valve vegetations can develop on damaged endothelium in patients with prior cardiac or valvular disease, up to 50% of the IE patients have no underlying heart disease and present with structurally normal cardiac valves.[16–19] Furthermore, the prognosis of these patients is often worse.[18,19] In this case, IE is hypothesized to originate from inflamed valves. Our group recently developed a mouse model that provides insights into the pathophysiology of endocarditis originating on intact cardiac valves subjected to acute local inflammation.[20] This model has revealed that *S. aureus* adhesion occurs differently on damaged versus inflamed valves.[20] To cause IE, bacteria have to not only adhere to cardiac valves, but they also need to thrive in the host environment to progress to advanced vegetations. We set out to investigate the role of neutrophils in this context, as they have been previously described to have both protective and pathological roles in immunothrombosis.[21]

As neutrophils are one of the first immune cells to enter a site of infection, bacteria need to bypass their immunological defense mechanisms to progress from single bacteria on cardiac valves to mature vegetations. In an attempt to combat an infection, neutrophils can release NETs (neutrophil extracellular traps), consisting of extracellular DNA strands bearing histones, granule proteins including MPO (myeloperoxidase) and defensins, and cytosolic proteins including calprotectin. When released into the extracellular space, NETs can restrict pathogens via their antimicrobial components.[22,23] These same microbicidal factors, however, also contribute to bystander effects by promoting uncontrolled thrombosis and subsequent tissue damage and inflammation.[24] As NETs both possess antibacterial and prothrombotic properties, it is unclear whether NETs diminish or enhance vegetation growth in IE.[25]

Prior studies on neutrophils and NETs in IE have focused on elucidating their role in artificial valve or damage-associated IE.[12–14,26] Immunohistochemical staining of valves from patients with IE predominantly caused by *Streptococci* revealed that extracellular DNA commonly colocalized with MPO, suggesting the presence of NETs inside these vegetations.[26] Bacteria entrapped within NET-like structures have also been identified inside rat IE vegetations,[12–14] where it was shown that DNase treatment reduced the vegetation size and colonizing bacteria numbers.[13,14] Whether this is an effect of NETs, however, still needs to be determined, as DNases can also degrade extracellular DNA released from bacteria and thus affect the bacterial biofilm. Moreover, these studies utilized models of IE with permanent catheter placement, more representative of IE on artificial structures. The role of NETs in native valve IE, therefore, remains unstudied.

One of the reasons why *S. aureus* is so proficient in causing endocarditis is its ability to manipulate both the coagulation cascade and innate and adaptive immunity via its arsenal of virulence factors.[25,27,28] *S. aureus* induces fibrin formation by activating prothrombin via the coagulases vWbp (von Willebrand factor binding protein) and Coa (staphylocoagulase). A Coa/vWbp-induced fibrin-rich layer was shown to shield off myeloid cells from entering bacteria-rich vegetation areas in mice.[29] In addition to activating the coagulation system, *S. aureus* is a master at evading the defense mechanisms of neutrophils and NETs. We recently reviewed the various mechanisms whereby *S. aureus* both promotes or hampers NET formation to its advantage.[25] These complex interactions are highlighted by the fact that, in vitro, *S. aureus* can both potently induce NET release and subsequently degrade them via secreted nucleases.[30,31] How *S. aureus* exactly manipulates NETs within IE vegetations, however, is unknown.

We, therefore, focused on characterizing the involvement of neutrophils and NETs in inflammation-induced endocarditis caused by various strains of *S. aureus*, by neutrophil depletion and a mouse model of impaired NET formation using neutrophil-selective PAD4

(peptidylarginine deiminase 4)-deficient mice. PAD4-deficiency has previously been shown to substantially reduce NET release in mice.[32–34] Finally, the impact of certain *S. aureus* virulence factors related to coagulation and immunothrombosis on NET formation and endocarditis development was assessed.

METHODS

Data Availability Statement

The data that support the findings of this study are available from the corresponding author upon reasonable request.

Animals

All animal experiments were reviewed and approved by the Animal Ethics Committee of KU Leuven (license numbers 040/2017, 189/2017). C57BL/6J male wild-type mice at 8 to 14 weeks of age were used for most experiments. Female mice were excluded due to reduced IE occurrence in this model. Before surgery, mice were anesthetized with a combination of ketamine (96 mg/kg body weight, Dechra, Northwich, United Kingdom) and xylazine (12 mg/kg body weight, VMD, Arendonk, Belgium) intraperitoneally. During follow-up, mice received buprenorphine (0.09 mg/kg body weight, Ceva, Libourne, France) twice daily. Well-being was assessed at least 3× per day with an in-house clinical scoring system that includes parameters for weight loss, body condition, physical appearance, respiratory changes, unprovoked activity, and behavioral responses to external stimuli. Mice were euthanized with pentobarbital (80 mg/kg, Vetoquinol, Aartselaar, Belgium) at experimental endpoints or when achieving a clinical score indicating they had reached predefined humane endpoints. Further information according to ARRIVE guidelines is available in the Supplemental Material.

Mouse Model of Inflammation-Induced Endocarditis

We employed a previously reported mouse model of IE that originates on inflamed valves.[20] To induce bacteremia, 2×10^6 colony-forming units (CFU) bacteria were injected intravenously via the tail vein. Next, the endothelium was locally activated at the aortic valves by insertion of a 32-gauge polyurethane catheter (Instech, Plymouth Meeting, PA) in the right carotid artery, and infusion of 200 mM histamine (Sigma-Aldrich, St. Louis, MO) at an infusion rate of 10 µL/min for 5 minutes locally at the aortic valve. The catheter was then immediately removed, and the surgical site was closed with surgical sutures. Mice were subsequently monitored for 1 to 3 days. Before euthanization, blood was withdrawn into 0.5 M EDTA (Sigma-Aldrich, St. Louis, MO) via retro-orbital puncture and plated on mannitol salt agar plates to define the levels of bacteremia by counting CFU. At experimental or humane endpoints, hearts were perfused with 0.9% sodium chloride (Baxter, Eigenbrakel, Belgium) followed by 4 % paraformaldehyde (Sigma-Aldrich, St. Louis, MO). Cryosections or paraffin sections of the aortic valve region were made at a thickness of 8 to 9 µm. To determine if endocarditis had developed, we performed a Brown-Hopps Gram staining (see Supplementary Methods) and analyzed 8 sections of aortic valves per mouse with a Zeiss Axiovert 200M inverted microscope equipped with a Zeiss HRc high resolution color camera. For more detailed methodology, we refer to our previous publication on this model.[20]

Bacterial Strains

We used *S. aureus* Newman (methicillin-susceptible) and USA300 (methicillin-resistant) as representative lab strains. Clinical strains of *S. aureus* and *Staphylococcus epidermidis* (*S. epidermidis*) were obtained from patient blood cultures. To study the effect of bacterial factors on progression of IE, we used mutants of *S. aureus* USA300 deficient in Δnuc (nucleases) and in both Coa and vWbp (ΔcoaΔvwb).[35,36] Bacteria were prepared grown overnight in Tryptic Soy Broth (Merck Millipore, Burlington, United Kingdom) at 37°C. After 2 washing steps in PBS (Gibco, Waltham, MA), optical densitometry (OD600) was used to quantify the bacteria which was then diluted to indicated concentrations before use. The administered amounts of bacteria were verified by plating serial dilutions on mannitol salt agar plates. All actions with *S. aureus* were performed according to enhanced biosafety level 2 (BSL2+) precautions, including use of personal protective equipment, a Biosafety laminar flow cabinet, and appropriate decontamination.

Neutrophil Depletion and Flow Cytometry

A recently described dual antibody-mediated method was used to deplete neutrophils in mice, which employs a rat antibody against Ly6G followed by a second injection of an anti-rat IgG κ antibody.[37] Mice were first intravenously injected with 8 µg/g rat In*Vivo*MAb anti-mouse Ly6G (Bio X Cell, Lebanon, NH) or 8 µg/g In*Vivo*MAb rat IgG2a isotype control (Bio X Cell, Lebanon, NH]). Twenty-four hours later, all mice received another intravenous injection at a dose of 4 µg/g of mouse IgG2a anti-rat IgGκ (Bio X Cell, Lebanon, NH). The endocarditis surgery was performed immediately after this second injection and mice were followed for 1 day. Keeping mice beyond the 1-day time point was not possible due to a majority of neutrophil-depleted mice reaching the humane endpoint on the first day after depletion.

Depletion of neutrophils was validated by flow cytometry. To this end, blood was withdrawn from mice under isoflurane (Piramal Critical Care, Bethlehem, PA) anesthesia by retro-orbital puncture into 0.5 M EDTA (Sigma-Aldrich, St. Louis, MO). This was performed before first antibody injections at day 1 (reference sample) and just before sacrifice at day 1 post-surgery. One part of whole blood was incubated with 9 parts of ammonium chloride potassium lysis buffer (Gibco, Waltham, MA) for 5 to 10 minutes at room temperature (RT) to lyse red blood cells. Subsequently, samples were centrifuged at 400*g* at RT for 5 minutes, washed twice with filtered 0.5 % BSA (bovine serum albumin, Roche, Mannheim, Germany) in PBS (Gibco, Waltham, MA), and incubated with 5 µg/mL anti-CD16/CD32 antibody (Biolegend, San Diego, CA) for 10 minutes at RT. After an additional centrifugation and washing step, cells were stained for 15 minutes at RT with the following fluorescently labeled antibodies: APC/Cy7-CD45 (clone 30-F11, 1 µg/mL), PerCP-Ly6G (clone 1A8, 1 µg/mL; Biolegend, San Diego, CA) and FITC-LY6B2 (clone 7/4, 10 µg/mL, Bio-Rad laboratories, Hercules, CA). After washing, 500 µl of cell suspension was transferred to polystyrene tubes containing 50 µl of CountBright absolute counting beads (Invitrogen, Waltham, MA) and analyzed on a Canto II Flow Cytometry analyzer (BD,

Franklin Lakes, NJ). Absolute cell counts were calculated as described in the manufacturer's protocol for the CountBright absolute counting beads.

Neutrophil-Selective PAD4 Knockout Mice

The role of NETs was determined using neutrophil-selective PAD4 knockout mice (MRP8Cre^{+}×PAD4$^{fl/fl}$), which are bred in-house and were generated from PAD4$^{fl/fl}$ and MRP8Cre^{+} (myeloid related protein 8, Cre recombinase expressing) strains purchased at the Jackson Laboratory (Bar Harbor, ME) which were backcrossed to a C57BL/6J background for at least 8 generations before intercrossing. PAD4 encodes an enzyme responsible for citrullination of histones; by deleting this gene NET formation is impaired. Neutrophil-selective PAD4 knockout mice and control mice (PAD4$^{fl/fl}$) received the above-described endocarditis procedure. Additionally, a separate set of experiments was performed to obtain sufficient infected thrombi for quantitative histological analysis in neutrophil-selective PAD4null mice, where bacteria were directly infused into the inflamed aortic valve via the catheter (in contrast to systemic injection), thus resulting in a more severe disease model.

Mouse Neutrophil In Vitro NET Assay

The degree of NET impairment in MRP8Cre^{+}×PAD4$^{fl/fl}$ strain was first validated in vitro using isolated peripheral blood neutrophils. Blood was withdrawn from isoflurane-anesthetized MRP8Cre^{+}×PAD4$^{fl/fl}$ or PAD4fl/fl mice via retro-orbital puncture into 2 volumes of PBS (Gibco, Waltham, MA) containing 15 mM EDTA (Strem Chemicals, Newburyport, MA) and 1 % low-endotoxin BSA (Carl Roth, Karlsruhe, Germany). Neutrophils were isolated using a density gradient.[38] Briefly, plasma-depleted blood was layered over a gradient of 78 %, 69 %, and 52 % Percoll PLUS (Sigma-Aldrich, St. Louis, MO), the 69 %/78 % interface was collected and the granulocyte pellet was resuspended in RPMI-1640 medium (Gibco, Waltham, MA) containing 10 mM HEPES. Cells were counted in a hemocytometer and purity was checked by flow cytometric detection of Ly6G+CD45+ cells using a BD FACSVerse flow cytometer. All isolations quantified in this paper achieved isolation purities of at least 90%. Next, neutrophils were incubated with 4 µM ionomycin (Invitrogen, Waltham, MA), *S. aureus* USA300 (multiplicity of infection 100), or the appropriate vehicle controls containing dimethyl sulfoxide (DMSO, Sigma-Aldrich, St. Louis, MO) or only RPMI-1640 medium (Gibco, Waltham, MA). After 3.5 hours at 37 °C, cells were fixed in 4 % paraformaldehyde (Sigma-Aldrich, St. Louis, MO) overnight. To assess the degree of NET formation, we stained for Ly6G to identify the cell membrane and for DNA with 2 µg/mL Hoechst 33342 (Invitrogen, Waltham, MA). We visualized 6 distinct fields of view with a Zeiss inverted Z1 Observer microscope equipped with a Zeiss 506 camera, and manually counted the neutrophils that were in various stages of NETosis based on nuclear shape and presence of extracellular DNA (stage 0: unstimulated neutrophils, stage 1: neutrophils with a delobulated nucleus, stage 2: neutrophils with a swollen nucleus or decondensed chromatin, stage 3: extruded NETs).

Human Neutrophil NET Assays

The ability of various bacterial strains to induce NETosis was assessed in an in vitro NET assay. Blood was withdrawn from healthy volunteers with informed consent (Ethical Commission of University Hospital Leuven) into EDTA vacutainers (BD, Franklin Lakes, NJ), and neutrophils were isolated using the MACSxpress Whole Blood Neutrophil Isolation kit (Miltenyi Biotec, Bergisch Gladbach, Germany), according to the manufacturer's protocol. Next, the collected neutrophils were washed with Hanks' Balanced Salt Solution (without calcium and magnesium, Invitrogen, Waltham, MA) and centrifuged at 500*g* for 10 minutes at 22 °C. The neutrophil pellet was resuspended in RPMI-1640 medium (with L-Glutamine and without phenol red, Gibco, Waltham, MA) supplemented with 10 mM HEPES (Gibco, Waltham, MA) and fetal calf serum (Gibco, Waltham, MA) heat inactivated (at 70 °C for 20 minutes) to a final concentration of 75 000 cells/ 50 µL. Subsequently, neutrophils were incubated with various bacterial strains (*S. aureus* Newman and USA300, clinical strain, and nuclease mutant of *S. aureus* and *S. epidermidis*) at a multiplicity of infection of 100 for 3 hours at 37 °C. To digest released NETs into quantifiable fragments, the cell culture supernatants were removed and 4 U AluI restriction enzyme in Tango buffer (Thermo Fisher Scientific, Waltham, MA) was added to the neutrophils for 20 minutes at 37 °C. Digested NET fragments were collected by thorough pipetting. The degree of NET induction was determined via a commercial H3Cit (citrullinated histone H3; clone 11D3) ELISA (Cayman Chemical, Ann Arbor, MI) according to the manufacturer's instructions.

In a separate set of experiments, isolated neutrophils were coincubated with bacteria and platelets. Platelet-rich plasma was first prepared by centrifuging citrate-anticoagulated (BD, Franklin Lakes, NJ) blood at 175 g for 15 minutes at 22 °C and collecting the supernatant. To isolate platelets, the platelet-rich plasma was supplemented with 2 µg/mL prostacyclin (Tocris Bioscience, Bristol, United Kingdom) and 0.02 U/mL apyrase (Sigma-Aldrich, St. Louis, MO) and centrifuged at 1000*g* for 10 minutes at 22 °C. The platelet pellet was subsequently washed in modified Tyrode HEPES buffer (containing 134 mM/L NaCl [VWR, Radnor, PA], 2.9 mM/L KCl, 0.34 mM/L Na_2HPO_4, 1 mM/L $MgCl_2$ (Merck Millipore, Burlington, United Kingdom), 12 mM/L $NaHCO_3$ and 20 mM/L HEPES (Sigma-Aldrich, St. Louis, MO), pH=7.4) supplemented with 0.1 % glucose (Merck Millipore, Burlington, United Kingdom), 0.35 % BSA (Roche, Mannheim, Germany), 0.02 U/mL apyrase (Sigma-Aldrich, St. Louis, MO), and 2 µg/mL prostacyclin (Tocris Bioscience, Bristol, United Kingdom). After an additional centrifugation step, the platelet pellet was resuspended to a final concentration of 6×10^8 platelets/mL in RPMI-1640 medium (with L-Glutamine and without phenol red) supplemented with 10 mM HEPES and fetal calf serum (70 °C heat inactivated). Platelets were incubated at a 200:1 ratio with neutrophils.

Immunofluorescence Staining

Various components of the coagulation and immunological defense system were visualized in the aortic valve sections obtained in the animal experiments. First, the sections were permeabilized with 0.1 % sodium citrate (Sigma-Aldrich, St. Louis, MO) and 0.1 % Triton X-100 (Sigma-Aldrich, St. Louis, MO) in PBS (Gibco, Waltham) for 10 minutes at 4 °C. After 3 washings steps with PBS, sections were incubated in blocking solution (PBS with 3 % BSA (Roche, Mannheim, Germany) and 10 % donkey serum (Sigma-Aldrich, St. Louis, MO) at 37 °C for 2 hours, again washed in PBS and incubated overnight

with specific primary antibodies in antibody dilution buffer (0.3 % BSA and 0.05 % Tween-20 (Sigma-Aldrich, St. Louis, MO) in PBS) at 4 °C. Bacteria were stained with 5 µg/mL rabbit anti–*S. aureus* antibody (Abcam, Cambridge, United Kingdom), neutrophils with 2.5 µg/mL rat anti-Ly6G antibody (Biolegend, San Diego, CA), and NETs with 2.5 µg/mL goat anti-myeloperoxidase antibody (MPO, R&D systems, Minneapolis, MN) and 2.5 µg/mL rabbit anti-Histone H3 (citrulline R2+R8+R17, H3Cit; Abcam, Cambridge, United Kingdom) or 2.5 µg/mL rabbit recombinant anti-Histone H3 (Abcam, Cambridge, United Kingdom) antibody. Platelets, fibrinogen, and VWF were visualized with 2.5 µg/mL rat anti-CD41 (Biolegend, San Diego, CA), 10 µg/mL sheep antifibrinogen (Bio-Rad laboratories, Hercules, CA) and 8.2 µg/mL rabbit anti-VWF (Dako, Agilent Technologies, Santa Clara, CA) antibodies, respectively. After washing 6× with PBS (Gibco, Waltham), 1.33 µg/mL of secondary antibodies (goat anti-rat IgG [H+L] AlexaFluor555, donkey anti-goat IgG [H+L] AlexaFluor555, donkey anti-rabbit AlexaFluor488 [H+L], or donkey anti-sheep IgG [H+L] AlexaFluor488, Invitrogen, Waltham) in antibody dilution buffer was added for 2 hours at RT. Hoechst 33342 (2.5 µg/mL, Invitrogen, Waltham, MA) was used to counterstain DNA. Background autofluorescence was minimized by adding 0.05% Sudan Black B (Sigma-Aldrich, St. Louis, MO) in 70 % ethanol for 7 minutes (NETs staining) or 0.1 % Sudan Black B for 20 minutes (platelet, fibrinogen, and VWF staining). For paraffin-embedded hearts, a deparaffination and antigen retrieval step (for the NETs staining 1× antigen retrieval reagent basic solution, R&D systems, Minneapolis, MN) was conducted before the permeabilization step. In addition to the above-described stainings, the Click-iT Plus TUNEL (terminal deoxynucleotidyl transferase dUTP nick-end labeling) Assay labeled with AlexaFluor647 (Invitrogen, Waltham, MA) was used for in situ apoptosis detection according to the manufacturer's instructions and a Martius Scarlet Blue staining was used to detect fibrin (see Supplementary Methods).

Stained sections were routinely visualized using a Zeiss Axioscan Z1 digital slide scanner at the VIB-KU Leuven LiMoNe Bio Imaging Core and areas with positive signal were quantified using ImageJ software (National Institutes of Health, Bethesda, MD). More detailed information on image acquisition and quantifications can be found in the Supplementary Methods.

Immuno-Electron Microscopy

NET release in vitro was visualized using immuno-scanning electron microscopy. Neutrophils were isolated as described above, seeded on poly-L-lysine coated coverslips (VWR, Radnor, PA) at a concentration of 1200 cells/µL and incubated with either 4 µM ionomycin (Invitrogen, Waltham) or bacteria (*S. aureus* USA300 wild-type and nuclease mutant, or *S. aureus* and *S. epidermidis* clinical strains) at an multiplicity of infection of 100 for 3 hours at 37 °C. Cells were fixed with 1% filtered electron microscopy (EM)-grade paraformaldehyde (Electron Microscopy Sciences, Hatfield), and permeabilized with 0.1% sodium citrate and 0.1% Triton X-100 in PBS (Gibco, Waltham, MA). Next, samples were blocked in 3% BSA and 20 % goat serum (Vector Laboratories, Burlingame), and stained for H3Cit with the primary rabbit anti-H3Cit (5 µg/mL, ab5103, Abcam, Cambridge, United Kingdom) antibody and a secondary 10 nm gold-conjugated goat F(ab')2 anti-rabbit IgG (H/L) antibody (1/20, Abcam, Cambridge, United Kingdom). Coverslips were additionally fixed in 2.5% filtered EM-grade glutaraldehyde (Sigma-Aldrich, St. Louis). After washing steps at 4 °C in 0.1 M filtered phosphate buffer (containing 0.1 M sodium phosphate monobasic monohydrate and 0.1 M sodium phosphate dibasic dihydrate, pH 7.4, Sigma-Aldrich, St. Louis) and 0.1 M filtered sodium cacodylate buffer (containing 0.1 M sodium cacodylate trihydrate, pH 7.6, Electron Microscopy Sciences, Hatfield, PA), the samples were incubated with 1% osmium tetroxide (Electron Microscopy Sciences, Hatfield, PA) in 0.1 M sodium cacodylate buffer for 1 hour. The coverslips were subsequently dehydrated in an ethanol gradient series, critical point dried, mounted on aluminum stubs, coated with 8 nm carbon, and imaged on a Zeiss Sigma scanning electron microscope (Carl Zeiss) at the Electron Microscopy platform of the VIB-KU Leuven Bio Imaging Core at an accelerating voltage of 2 kV and high vacuum, or at 7.5 kV and 10 Pa chamber pressure. Images were acquired using the secondary electron signal for morphological surface details or backscatter electron signal for identification of gold labels. Pseudocoloring of the gold particles was done with the thresholding tool in the Microscopy Image Browser software (version 2.81, Electron Microscopy Unit, University of Helsinki, Finland).

Statistical Analyses

Statistical analyses were conducted with GraphPad Prism version 9.3.1 (GraphPad Software, La Jolla). Continuous data are represented by median and interquartile range and significance was determined by Mann-Whitney test for comparison of 2 groups or by Kruskal-Wallis test with Dunn post test for >2 groups. For categorical variables, frequencies are reported together with results of Fisher Exact tests. All statistical analyses were evaluated at the 0.05 significance level.

RESULTS

Large Infiltrates of Neutrophils Surround Aortic Valve Vegetations Rich in Bacteria, von Willebrand Factor, Platelets, Fibrinogen, and Fibrin

After inducing IE, a proportion of mice developed endocarditis (here defined as infected vegetations/thrombi), while others developed no thrombi or sterile thrombi without bacteria at day 3 (Figure 1A). Compared with sterile thrombi, infected vegetations were typically larger and were surrounded by a cellular infiltrate (*) in the aortic wall (Figure 1A). This infiltrate consisted mainly of Ly6G+ cells (**), which is a specific marker of mouse neutrophils (Figure 1B). Further characterization of components of the coagulation system revealed that both infected and sterile thrombi contained VWF, fibrinogen, CD41+ platelets, and fibrin to a similar extent (Figure 1C through 1E). These components were absent in mice without vegetations. In comparison to IE lesions, more platelets and fibrinogen were present in sterile thrombi (Figure 1D). Quantitative analyses confirmed all qualitative observations (Figure S1).

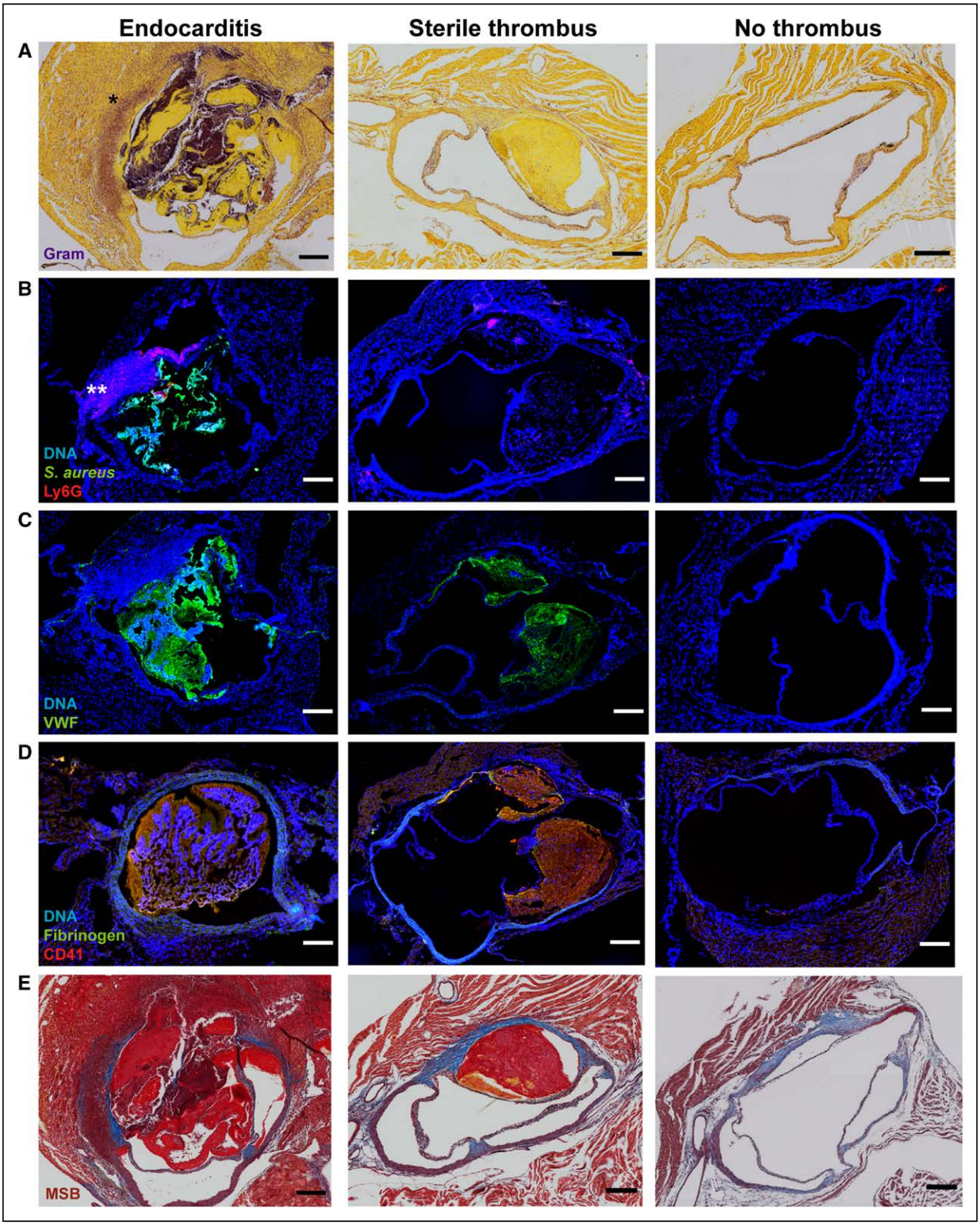

Figure 1. Histological characterization of advanced endocarditis vegetations and sterile thrombi.
Various components were characterized in mice with infective endocarditis (n=11), sterile thrombi (n=7), or without thrombi (n=7), induced by the clinical strain of *Staphylococcus aureus* at day 3. Representative images of these components in each group are shown in **A**–**E**. **A**, Brightfield images of a Brown-Hopps Gram stain with bacteria seen in purple and asterisks (*) indicating large cellular infiltrates in the surrounding aortic wall. **B**–**D**, Fluorescence images of *S. aureus* (green) and neutrophil-specific marker Ly6G (red, **B**); VWF (von Willebrand factor, green, **C**); and platelet CD41 (red) and fibrinogen (green; **D**). DNA is identified by Hoechst 33342 staining, depicted in blue. Double asterisks (**) indicate large infiltrates of neutrophils in the surrounding aortic wall. **E**, Martius Scarlet Blue (MSB) staining that detects fibrin in red. Scale bars represent 200 μm.

Neutrophils Protect Against IE

The above-described results showed that neutrophils were abundantly present in mice with endocarditis vegetations. To begin dissecting their functional role, we depleted neutrophils in mice by subsequent injections of antibodies against Ly6G and rat IgG2aκ and then performed the surgical procedure to induce IE (Figure 2A). After 1 day, significantly more mice developed inflammation-induced endocarditis in the neutrophil depletion group (Figure 2B-D), which was observed in mice infected with *S. aureus* USA300 (52% versus 19%), a clinical *S. aureus* IE strain (31% versus 0%) and the less virulent, coagulase-negative *S. epidermidis* (50% versus 0%). Furthermore, neutrophil-depleted mice had increased levels of systemically circulating bacteria indicative of bacteremia (Figure 2E through 2G). In accordance with these findings, all thrombi in neutrophil-depleted animals contained bacteria, and no sterile thrombi were present (Figure 2H through 2J). To determine if neutrophils resulted in these sterile thrombi by clearing bacteria inside the vegetation, mice underwent the endocarditis surgery without receiving bacteria. Even when they were not infected, 4 out of 9 mice (44%) still developed sterile thrombi (data not shown), indicating that thrombus formation in this model can occur without the presence of *S. aureus*.

Additionally, we validated the antibody-mediated neutrophil depletion method by flow cytometry (Figure S2) and further characterized the IE vegetations by immunofluorescence staining (Figure S3). The absence of Ly6G+/Ly6B+ cells at endpoint in the neutrophil depletion group revealed successful antibody injections (Figure S2E). The amount of Ly6G−/Ly6B+ cells at endpoint (296.4 [219.9–428.9] cells/μL) was not equal (P=0.030) to the amount of Ly6G+/Ly6B+ cells before depletion (392.3 [278.8–716.5] cells/μL), supporting that this method effectively depleted neutrophils (Figure S2E and S2F). Fluorescence staining of tissue for neutrophil markers confirmed that neutrophil-depleted mice contained less MPO and Ly6G at the aortic valve or within thrombi (Figure S3A through S3D). Staining for the NET-specific marker H3Cit also showed the absence of neutrophils undergoing NET formation (Figure S3A and S3B, S3G). There were no differences in thrombus size or other markers related to IE (Figure S3A, S3B, S3E, S3F, S3H through S3J).

Neutrophils at Early Stages of NET Formation and Released NETs Are Present in *S. aureus* Endocarditis Lesions

In an attempt to constrain an infection, neutrophils can release NETs. Given the strong presence of neutrophils in IE, and that *S. aureus* is a potent NET inducer,[25] we investigated the presence of NETs in IE development.

First, the ability of different strains of *S. aureus* to induce NET formation was assessed in an in vitro NET release assay where we quantified NET fragments in supernatants before or after digestion with the restriction enzyme AluI. An increase in signal between non-digested controls and digested samples indicates release of NETs. Incubation of neutrophils from healthy volunteers with *S. aureus* USA300, *S. aureus* Newman, and a clinical *S. aureus* IE strain induced the release of H3Cit-positive NETs (Figure 3A). In comparison to nonstimulated (vehicle) neutrophils, the clinical *S. aureus* strain induced significantly more NET formation (Figure 3B). H3Cit induced by *S. aureus* USA300, Newman, and the clinical strain could still be detected in the absence of the digesting enzyme AluI, (blue dots Figure 3A), indicative that the release of nucleases from *S. aureus* digested NETs into detectable fragments in our assay setup independent of addition of AluI. When neutrophils were incubated with *S. aureus* USA300 deficient in nuclease (*S. aureus* Δnuc), a virulence factor of *S. aureus* that degrades the DNA backbone of NETs, we could detect significantly increased NET fragments only in the conditions with digestion by AluI (Figure 3A and 3B). Interestingly, *S. epidermidis*, a coagulase-negative Staphylococcus, did not induce NET formation (Figure 3A and 3B). In the presence of platelets, *S. aureus* USA300 and the clinical *S. aureus* strain significantly enhanced NETosis in comparison to neutrophils incubated with vehicle, whereas *S. aureus* Newman or *S. epidermidis* did not (Figure 3C and 3D). To validate that the H3Cit detected by the ELISA in digested NET fragment samples originated from NETs, we performed scanning electron microscopy on stimulated neutrophils incubated with a primary antibody against H3Cit and a gold-conjugated secondary antibody. Immuno-scanning electron microscopy confirmed the induction of NETs by the clinical *S. aureus* IE strain (Figure 3E and 3I), by *S. aureus* Δnuc (Figure 3F and 3J), and by the calcium ionophore ionomycin included as a positive control condition to set EM instrument configuration (Figure 3G and 3K). In the presence of *S. epidermidis*, phagocytosing neutrophils, but no NETs, were detected (Figure 3H and 3L).

NETs are typically characterized by the colocalization of extracellular DNA, a non-nuclear neutrophil protein such as MPO, and presence of citrullinated histones. Fluorescence staining for these markers revealed the presence of NETs and neutrophils undergoing early-stage NETosis in mice with IE induced by different strains of *S. aureus* (Figure 4A through 4C). Large infiltrates of MPO- or H3Cit-positive cells were also present in the wall of the aorta. Mice with inflammation-induced infected vegetations had significantly more MPO and H3Cit at day 3 compared with those without any lesion (Figure 4D and 4E). This indicates that the inflammatory process in IE extends beyond the thrombus itself.

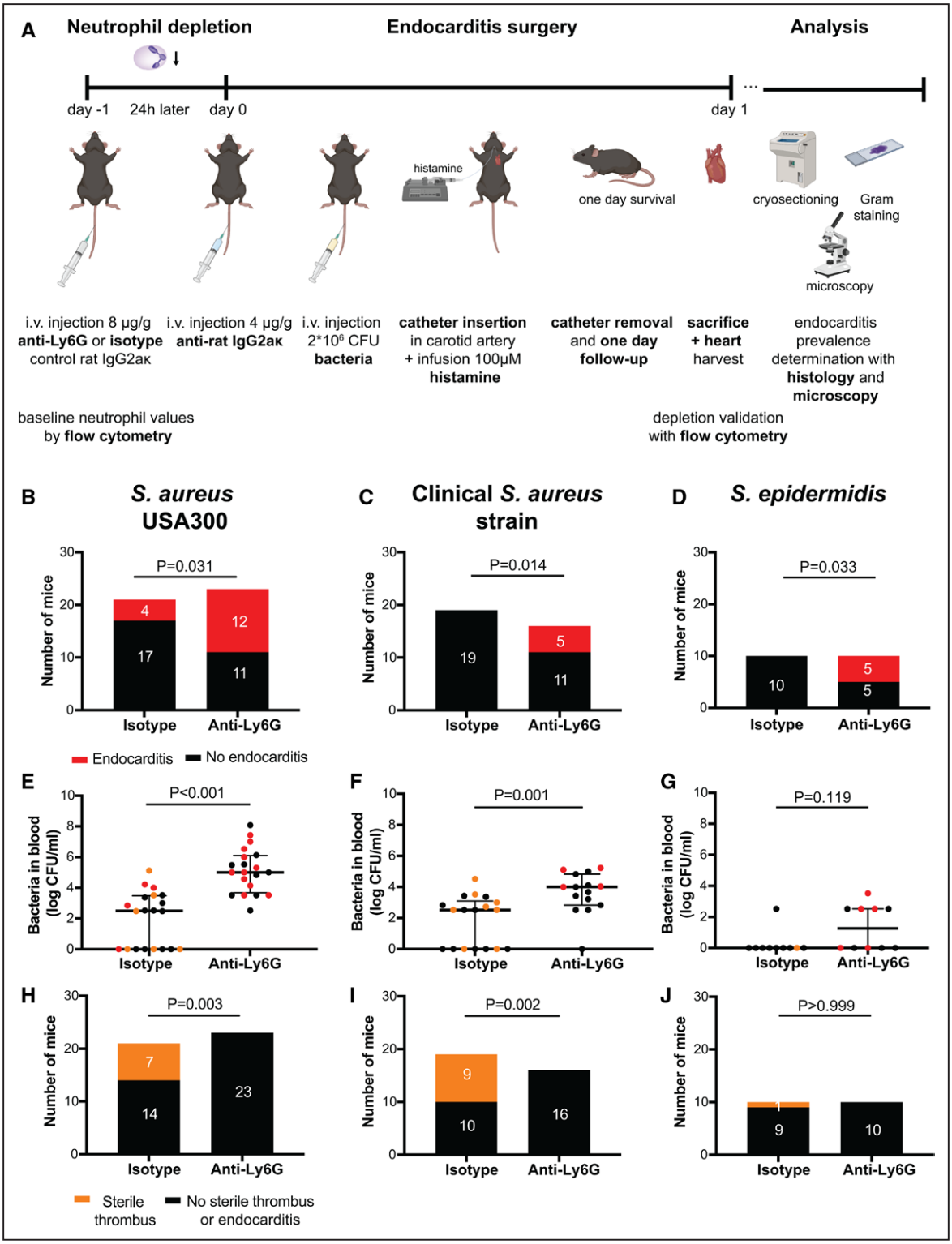

Figure 2. Neutrophils protect against infective endocarditis.
Following neutrophil depletion, mice underwent endocarditis surgery and were monitored for 1 day. **A**, Schematic overview of the neutrophil depletion experiment design (made with Biorender.com). **B**–**D**, Proportions of mice that developed infective endocarditis (red) at day 1 in neutrophil-depleted (anti-Ly6G) mice compared with isotype-control mice, infected with the methicillin-resistant strain of *Staphylococcus aureus* USA300, a clinical endocarditis isolate *S. aureus* strain and a coagulase-negative strain (*Staphylococcus epidermidis*). **E**–**G**, Bacteremia levels at end point with corresponding median (interquartile range) in neutrophil-depleted (n=20, 14, 10) and isotype-control (n=20, 18, 10) mice. Endocarditis vegetations are depicted in red, sterile thrombi in orange, and no thrombus in black. **H**–**J**, Proportions of mice that developed sterile thrombi (orange) in neutrophil-depleted mice compared with isotype-control mice. Fisher Exact (**B**–**D**, **H**–**J**) or Mann-Whitney tests (**E**–**G**) were conducted. CFU indicates colony-forming units; and Ly6G, lymphocyte antigen 6 complex locus G6D.

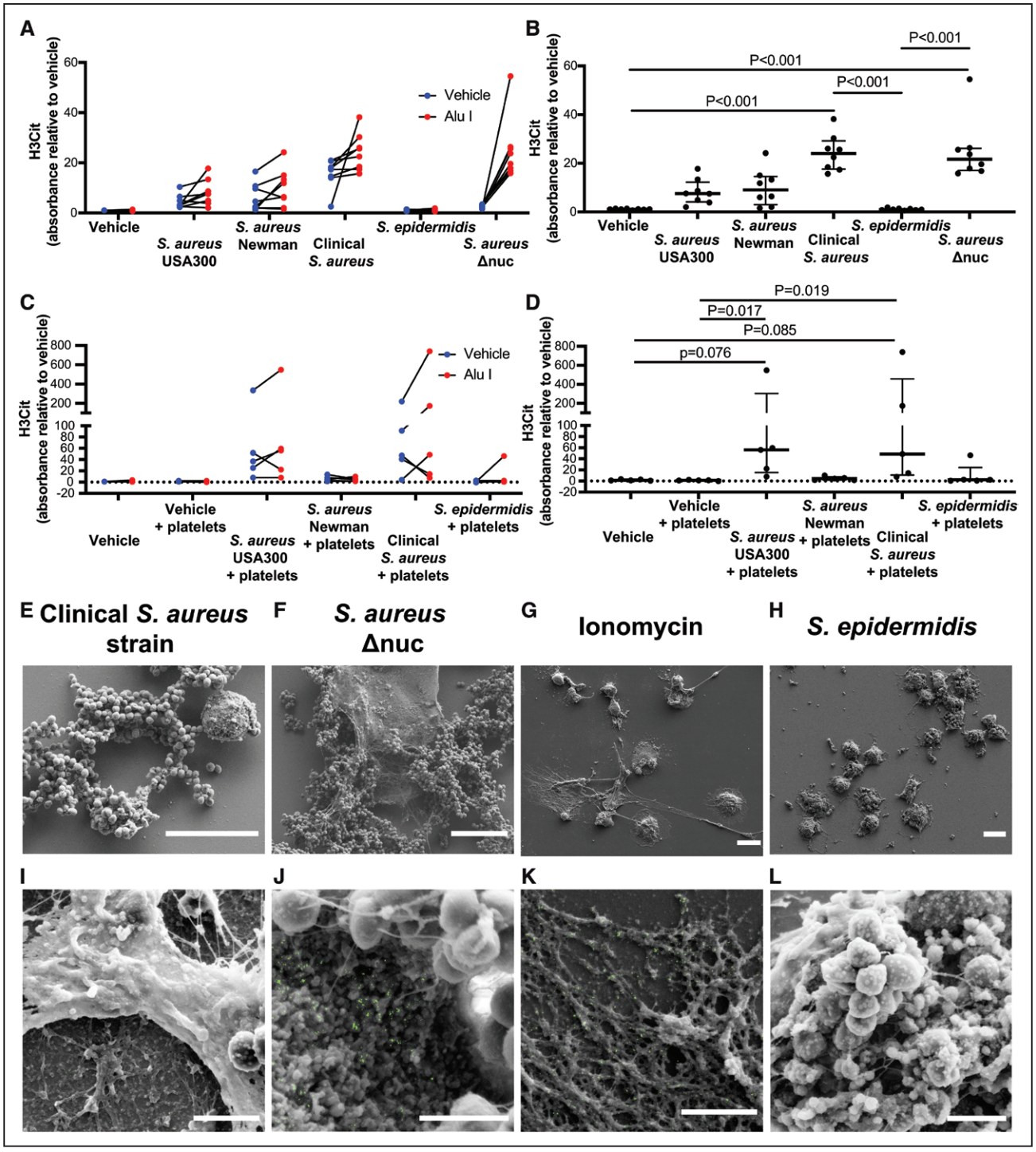

Figure 3. Different strains of *Staphylococcus aureus* induce NETs (neutrophil extracellular traps), whereas a less virulent coagulase-negative Staphylococcus strain does not induce NETosis (the process of NET formation).

A–**D,** In an in vitro NET release assay, isolated neutrophils (75 000 cells per well) from healthy volunteers were incubated with various bacterial strains (multiplicity of infection [MOI] 100) for 3 hours, and formed NETs were digested to smaller fragments with AluI (4 U) and measured in cell culture supernatants for H3Cit (citrullinated histone H3). **A, C**, H3Cit absorbances relative to nonstimulated (vehicle-treated) of digested (AluI, red) compared to nondigested (vehicle, blue) samples in the absence (n=8, **A**) or presence of platelets (6×10^8 cells/mL, n=5, **C**). **B** and **D**, H3Cit absorbances relative to vehicle of AluI digested samples with corresponding median (interquartile range) in the absence (n=8, **B**) or presence of platelets (n=5, **D**). Each single dot represents a single donor. Significance was determined by Kruskal-Wallis test with Dunn post test (**B**, **D**). **E**–**H**, Overview scanning electron microscopy (SEM) images (secondary electron signal) of NETs formed in the in vitro NET release assay. Scale bar equals 10 µm. **I**–**L**, Detailed secondary electron images of NETs incubated with a rabbit anti-H3Cit and a gold-conjugated anti-rabbit antibody. Gold particles were identified on corresponding backscatter electron SEM images and are depicted in green. Scale bars represent 500 nm. Due to different degrees of charging, a different threshold for the gold particles was used in **K** than in **I**, **J**, and **L**. Complete *P* values for data presented in **B** and **D** are available in Table S1 and S2, respectively. Δnuc indicates nucleases.

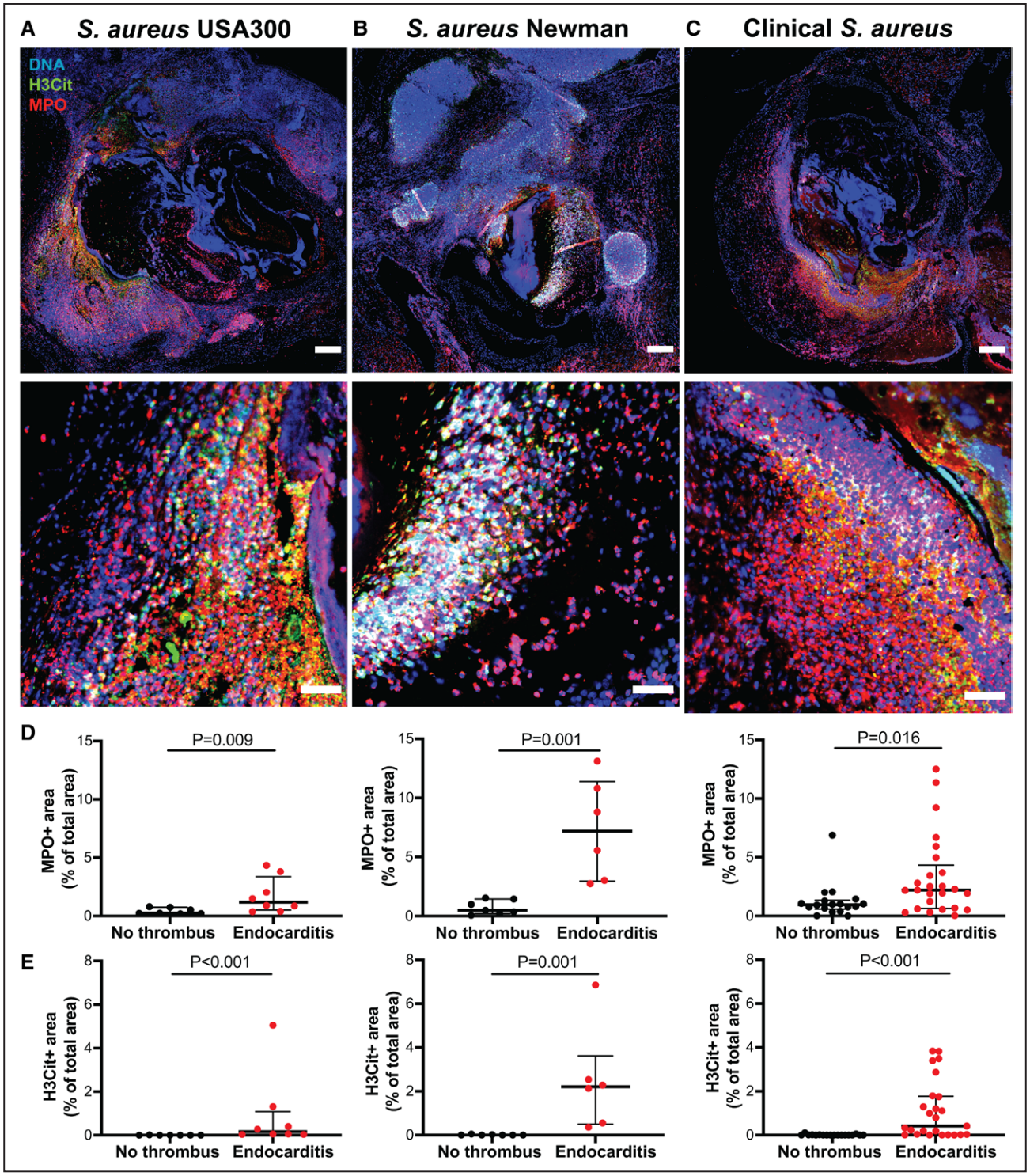

Figure 4. Neutrophils undergoing NET (neutrophil extracellular trap) formation and released NETs are present in mice with *Staphylococcus aureus*–induced endocarditis.

A–**C**, Fluorescence microscopy images of the following NET markers: H3Cit (citrullinated histone H3, green), MPO (myeloperoxidase, red), and DNA (blue) in inflammation-induced endocarditis vegetations infected with *S. aureus* USA300 (n=8, **A**), Newman (n=6, **B**) or a clinical *S. aureus* endocarditis strain (n=25, **C**) at day 3. Scale bar of upper and lower panels equals 200 µm and 50 µm respectively. In **C**, a different color balance threshold was used for MPO than in **A** and **B**. **D** and **E**, Quantifications of MPO (**D**) and H3Cit (**E**) positive area in mice with infective endocarditis (red dots, n=8, 6, 25) compared with mice without a vegetation (black dots, n=7, 7, 18). Median (interquartile range) are represented, and Mann-Whitney tests were used to test for statistical significance (**D** and **E**).

PAD4-Mediated NET Formation Does Not Protect Against IE

One potential explanation for the observed effect of neutrophil depletion could be the absence of NET formation. The impact of NETs on the progression of IE on inflamed valves was therefore investigated in neutrophil-selective PAD4 knockout (MRP8Cre^{+}×PAD4$^{fl/fl}$) animals. NETosis can be described in 4 stages with stage 0 representing intact neutrophils with lobulated nucleus, stage 1 nucleus delobulation, stage 2 nuclear swelling, and stage 3 extracellular release of DNA (Figure 5A). Neutrophils isolated from these knockout mice formed fewer NETs via PAD4 after stimulation with ionomycin or *S. aureus* USA300 than control animals (Figure 5B through 5D). Instead of releasing NETs (stage 3), more neutrophils were still in stage 1 (delobulated nuclei) and 2 (decondensed nuclei) of NETosis in the presence of ionomycin and in stage zero (lobulated nuclei) when incubated with *S. aureus* (Figure 5B). After validating this mouse strain for NET impairment in vitro, we infected neutrophil-selective PAD4 knockout (MRP8Cre^{+}×PAD4$^{fl/fl}$) and control mice (PAD4$^{fl/fl}$) with the clinical *S. aureus* strain, performed the endocarditis surgery (Figure 5E) and followed them up for 3 days to examine IE occurrence and progression (Figure 5F through 5I). The proportion of mice that developed IE was not significantly different (P=0.570) between those with impaired (35%) and intact (44%) NETosis (Figure 5F). There were also no differences in the presence of sterile thrombi (30% vs 28%, P>0.999; Figure 5G). Additionally, no significant differences in bacteremia levels (log 2.67 [0–4.25] versus log 3.67 [0–5.60] CFU/mL) and survival between neutrophil-selective PAD4 knockout and control mice were detected (Figure 5H and 5I). Similar results were detected in a short-term endocarditis model, where mice were intravenously injected with *S. aureus* USA300 and survived for 1 day, and a more severe endocarditis model, where bacteria were infused via the catheter for direct local administration to the activated aortic valve (Figure S4A through S4F). The size and the composition (MPO, bacteria, Ly6G, platelets, fibrinogen, and VWF) of the infected vegetation did also not significantly differ between mice with impaired and normal NET formation (Figure S5A through S5L). In the 1-day catheter delivery model, significantly less H3Cit was present in knockout compared to control mice (Figure S5N).

Large Cellular Infiltrates in the Surrounding Aortic Wall Promote Tissue Destruction in IE

As described above, inflammation-induced endocarditis vegetations were mostly surrounded by large cellular infiltrates in the aortic wall. Different strains of *S. aureus*–induced leukocyte infiltrates in IE and these were almost completely absent in sterile thrombi (Figure 6A and 6B). Staining heart valves with a Click-iT TUNEL assay revealed the presence of large apoptosis-positive areas in the surrounding vasculature of mice infected with *S. aureus* USA300, *S. aureus* Newman and the clinical *S. aureus* strain (Figure 6C). Although vegetations infected with the clinical *S. aureus* strain had significantly smaller areas of extraluminal leukocyte infiltration compared to *S. aureus* Newman, there was no difference in the TUNEL+ area between the 3 strains of *S. aureus* (Figure 6D and 6E). Interestingly, the area of extraluminal leukocyte infiltration significantly correlated with the TUNEL-positive area (Figure 6F). These leukocyte infiltrates and apoptosis-positive areas were still similarly present in mice with impaired NET formation (Figure S5O through S5T).

Staphylocoagulases Prevent NETs From Constraining Bacterial Infection and Promoting Tissue Destruction

The observation that mice with impaired NET formation did not develop less endocarditis could be due to *S. aureus* nucleases degrading NETs, rendering their potential antimicrobial or prothrombotic effects ineffective. Therefore, we tested a nuclease mutant of *S. aureus* USA300 (*S. aureus* Δnuc) in our 3-day IE model. However, wild-type mice infected with the nuclease mutant did not develop less endocarditis (8% versus 8%, P>0.999) or more sterile thrombi (50% versus 83%, P=0.190) compared with *S. aureus* USA300 (Figure 7A and 7B). Accordingly, bacteremia levels (log 3.28 [0–3.60] versus log 2.52 [0–4.67] CFU/mL) and survival were not different between *S. aureus* Δnuc and USA300 (Figure 7C and 7D). Large extraluminal infiltrates of Ly6G (1.61%, n=1), MPO (1.48%, n=1), and H3Cit (4.59%, n=1) positive areas were still present in mice infected with *S. aureus* Δnuc.

Recent evidence showed that *S. aureus*–induced fibrin can shield off myeloid cells from entering IE vegetations in an animal model involving permanent placement of a suture at the aortic valve.[29] As leukocyte infiltrates were similarly present in mice with impaired NET formation and in mice injected with *S. aureus* Δnuc, we investigated if disrupting this fibrin shield produced by *S. aureus* could impact IE progression, especially with respect to neutrophils and neutrophils releasing NETs. To this end, mice were infected with *S. aureus* USA300 doubly deficient in Coa and vWbp (ΔcoaΔvwb), the 2 virulence factors responsible for the coagulase activity of *S. aureus*. Although mice infected with *S. aureus* ΔcoaΔvwb did not develop less IE (35% versus 37%, P>0.999) or more sterile thrombi (50% versus 48%, P>0.999), these mice had significantly diminished bacteria levels in their blood (log 0 [0–0] versus log 2.52 [0–4.73] CFU/mL) and improved survival (Figure 7E through 7H). Moreover, mice infected with *S. aureus* ΔcoaΔvwb had significantly smaller areas of extraluminal infiltrate (Figure 8A and 8E)

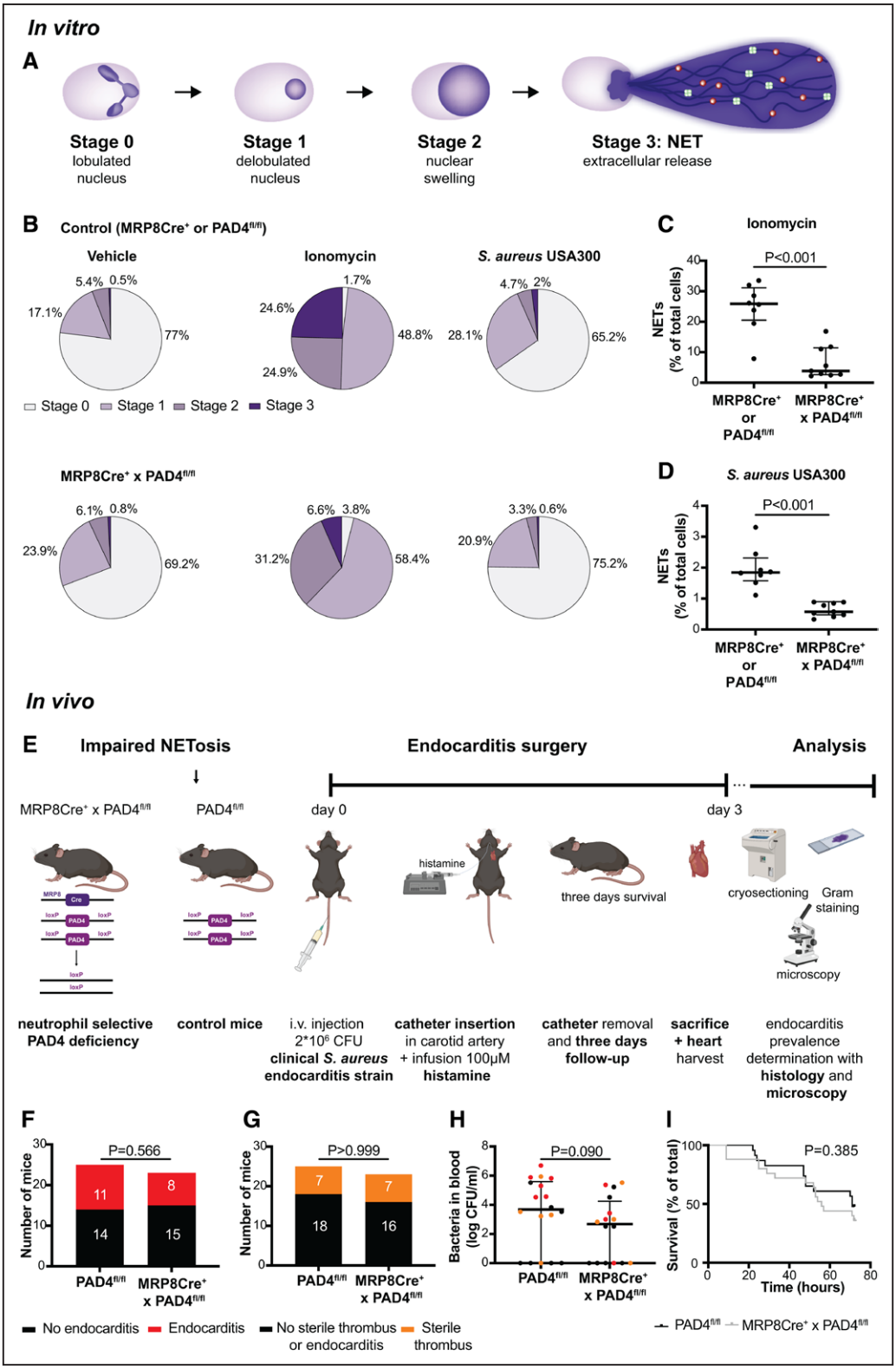

Figure 5. PAD4 (peptidylarginine deiminase 4)-mediated NET (neutrophil extracellular traps) release neither protects against nor promotes infective endocarditis.

A–**E**, In vitro assay: neutrophils were isolated from control (MRP8^{+} or PAD4$^{fl/fl}$) or neutrophil-selective PAD4 knockout mice (MRP8Cre^{+}×PAD4$^{fl/fl}$), incubated with *Staphylococcus aureus* USA300 or ionomycin, and the different stages of NETosis were assessed according to nuclear morphology. **A**, Schematic overview of the different stages of NET formation. **B**, Percentage of cells at various NETosis stages in control (average of n=8) and neutrophil-selective PAD4 knockout mice (average of n=9). **C** and **D**, Percentage of NETs induced by ionomycin (**C**) and *S. aureus* USA300 (**D**) in neutrophil-selective PAD4 knockout (n=9) mice compared with controls (n=8). (*Continued*)

and of TUNEL-positive areas outside the vessel wall (Figure 8B and 8F) in comparison to mice infected with *S. aureus* USA300. They did not, however, have statistically significant differences in fibrin content and size of the thrombi (Figure S6A and S6B). The TUNEL or apoptosis-positive area positively correlated with the H3Cit positive area (Figure 8G), the infiltrate area (Figure S6C), and the *S. aureus*, MPO, and Ly6G-positive area (Figure S6D through S6F) in the adjacent vessel wall area, and negatively correlated with the H3Cit positive area inside the thrombus (Figure S6G). More detailed characterization of vegetations induced by *S. aureus* ΔcoaΔvwb revealed that these contained less bacteria in the surrounding aortic wall (Figure 8C and 8H) and more H3Cit inside the thrombus (Figure 8D and 8I). The H3Cit signal inside the vegetation negatively correlated with the signal for bacteria outside the thrombus (Figure 8J). These data indicate that in the absence of staphylocoagulases, NET-releasing neutrophils are able to enter the thrombus and may thus be able to better constrain bacterial infection and tissue damage. To confirm this finding, we infected neutrophil-selective PAD4 knockout (MRP8Cre^{+}×PAD4$^{fl/fl}$) and control (PAD4$^{fl/fl}$) mice with *S. aureus* ΔcoaΔvwb, performed the endocarditis surgery, and monitored them for 3 days. *S. aureus* ΔcoaΔvwb infected mice with impaired NET formation developed endocarditis in 36% of cases as compared to 6% of wild-type animals with intact NET formation capability (P=0.054), equally developed sterile thrombi (36% versus 56%, P=0.450), and had similar bacteremia levels (log 0 [0–0] versus log 0 [0–2.524] CFU/mL) and survival rates (Figure S7). However, neutrophil-selective PAD4 knockout mice with *S. aureus* ΔcoaΔvwb-induced endocarditis had significantly larger areas of extraluminal infiltrates and of TUNEL-positive areas outside of the vessel wall in comparison to control mice with *S. aureus* ΔcoaΔvwb-induced endocarditis (Figure 8A and 8B, 8E and 8F). These mice with impaired NET formation and *S. aureus* ΔcoaΔvwb-induced endocarditis also had more bacteria, Ly6G, and MPO in the surrounding aortic wall (Figure 8C and 8D, 8H, 8K and 8L), and less H3Cit inside the thrombus (Figure 8D and 8I). In summary, in the absence of staphylocoagulases, NETs play an essential role in constraining the infection and hampering tissue damage in mice with IE.

DISCUSSION

S. aureus–mediated endocarditis is a unique disease that involves a complex interplay between the infecting microbe and innate immune defense mechanisms afforded by neutrophils and clotting factors. The complexity of this interplay is further deconvoluted in this study. We report that NETs are largely ineffective against inflammation-induced endocarditis driven by *S. aureus*. This likely occurs because neutrophil entry into thrombi is shielded with fibrin produced by *S. aureus* through its coagulases, as has been previously demonstrated.[29]

Depleting neutrophils in mice revealed that the neutrophil host defense mechanisms minimize progression in *S. aureus* inflammation-induced IE, as neutrophil depletion increased IE occurrence and led to persistent bacteremia. Infection with *S. aureus* provoked the recruitment and accumulation of large infiltrates of neutrophils and neutrophils releasing NETs surrounding the infected thrombus, presumably in a failed attempt to clear the infection. Our research suggests a role for staphylocoagulases in evading the defense mechanisms of neutrophils in IE. Since *S. aureus* USA300-induced endocarditis continued to develop in the presence of neutrophils but was exacerbated in the absence of neutrophils, we concluded that neutrophils only partially prevented endocarditis development.

One of the neutrophil's immune defense mechanisms is the release of NETs. By detecting H3Cit with ELISAs, immuno-electron, and immunofluorescence microscopy, we identified and quantified the presence of NETs in an in vitro *S. aureus*–induced NET release assay and in murine vegetations. Multiple *S. aureus* toxins have been shown to induce NETs in vitro.[14,30,39–44] Our assays confirmed the ability of *S. aureus* USA300 and Newman to induce NETs, and showed that a clinical IE *S. aureus* strain and *S. aureus* Δnuc were the most potent NET inducers. However, neutrophils incubated with *S. epidermidis* released almost no NETs. The ability of coagulase-negative strains, such as *S. epidermidis*, to induce NETs has remained a matter of debate.[39,45,46] In parallel to our in vitro findings, *S. aureus* USA300, Newman, and the clinical strain induced dense areas of NETs and NET-releasing neutrophils in mice with IE.

Inducing IE in neutrophil-selective PAD4 knockout mice reduced NET release but did not diminish or enhance endocarditis development, nor did it alter bacteremia levels and survival rates. This indicates that PAD4-mediated NET formation neither prevents nor aggravates endocarditis progression. A previous study showed that DNase administration reduced vegetation size in a damage-induced rat-model with *S. aureus* and *Streptococcus mutans*, suggesting a detrimental role of extracellular DNA in the pathophysiology of IE.[13,14] Our data indicate that this extracellular DNA is not likely of NET origin. DNases

Figure 5 Continued. Medians (interquartile ranges) are shown. **E**, Schematic overview (created with Biorender.com) of endocarditis experiments performed in neutrophil-selective PAD4 knockout and control mice. **F** and **G**, Proportions of mice that developed inflammation-induced endocarditis (red, **F**) or sterile thrombi (orange, **G**) at day 3 in neutrophil-selective PAD4 knockout mice compared with control mice. **H**, Bacteremia levels at end point with corresponding median (interquartile range; n=18, 16). **I**, Survival graph of neutrophil-selective PAD4 knockout (black, n=23) and control mice (gray, n=25). Mann-Whitney (**C** and **D, H**), Fisher Exact (**F** and **G**) or log-rank (Mantel-Cox) test (**I**). CFU indicates colony-forming units; MRP8, myeloid related protein 8; and NETosis, the process of NET formation.

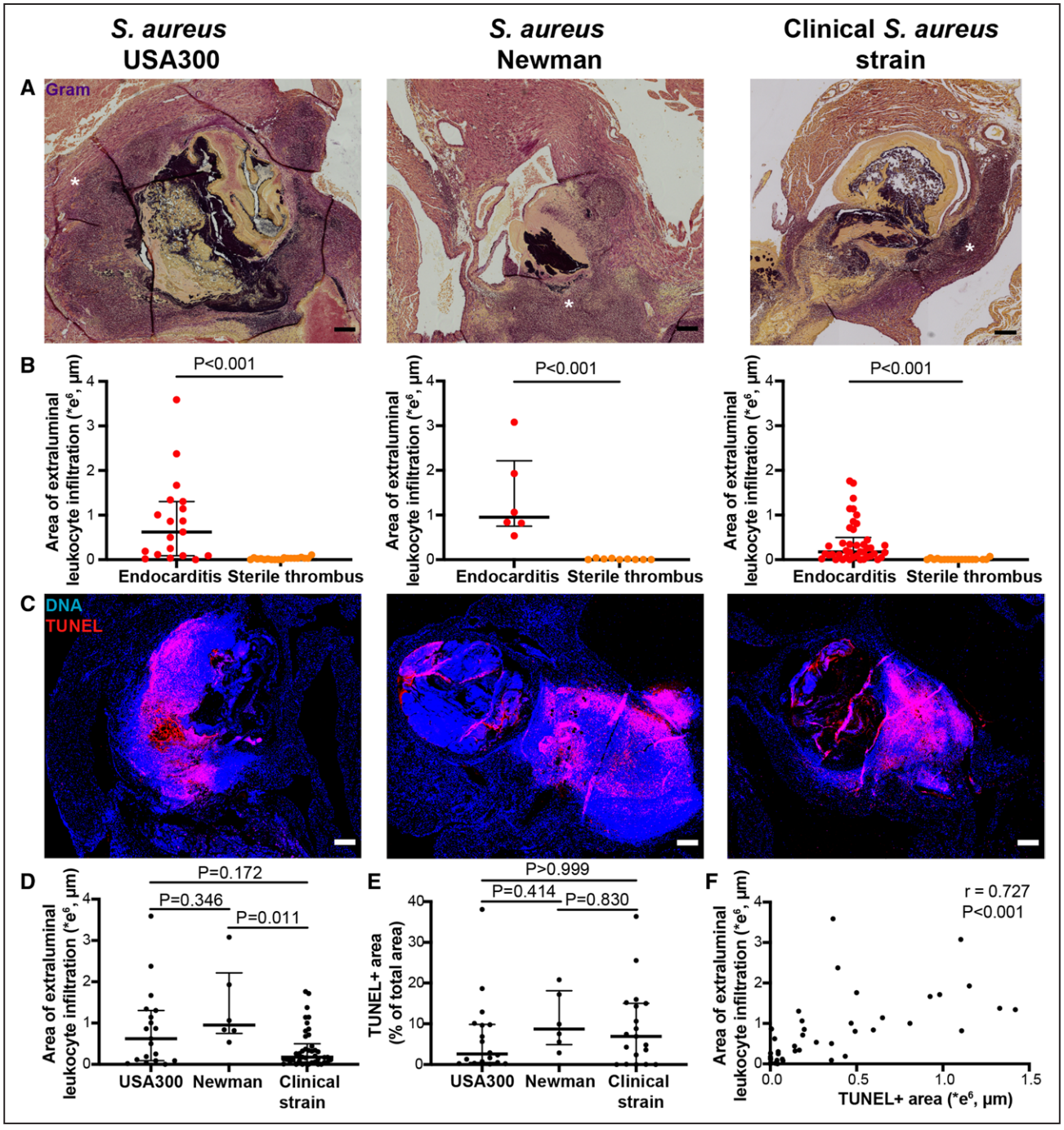

Figure 6. Large cellular infiltrates in the surrounding aortic wall promote tissue destruction.
A, Brown-Hopps Gram stain of endocarditis vegetations induced by *Staphylococcus aureus* USA300 (n=19), *S. aureus* Newman (n=6), or the clinical *S. aureus* strain (n=42), depicting large cellular infiltrates (*) in the surrounding vasculature. **B**, Quantifications of the extraluminal leukocyte infiltration area in infected (red dots, n=19, 6, 42) compared with sterile (orange dots, n=18, 9, 19, respectively) thrombi. **C**, Click-iT Plus TUNEL (terminal deoxynucleotidyl transferase dUTP nick-end labeling) assay stained images of endocarditis vegetations (n=18, 6, 19, respectively), depicting apoptotic cells in red. DNA is stained with Hoechst 33342 in blue. **D**, Comparison of the extraluminal leukocyte infiltration area between the 3 different strains of *S. aureus* (n=19, 6, 42, respectively). **E**, Quantification of the TUNEL-positive area outside the thrombus in mice with infected vegetations caused by the 3 different strains of *S. aureus* (n=18, 6, 19, respectively). **F**, Spearman correlation between the leukocyte infiltration area and TUNEL-positive area located outside the infected vegetation caused by the 3 different strains of *S. aureus* (n=43). Scale bar represents 200 µm. Median (interquartile range) are shown and significance level is evaluated by Mann-Whitney (**B**) or Kruskal-Wallis test with Dunn post tests (**D** and **E**).

are also able to degrade extracellular DNA from bacterial biofilms and consequently may resolve vegetations independently of NET involvement.[47,48] NET formation in IE could also be regulated by other mediators than PAD4. It has been shown that in later stages of *S. aureus*–induced NET formation, NET release is driven by reactive oxygen

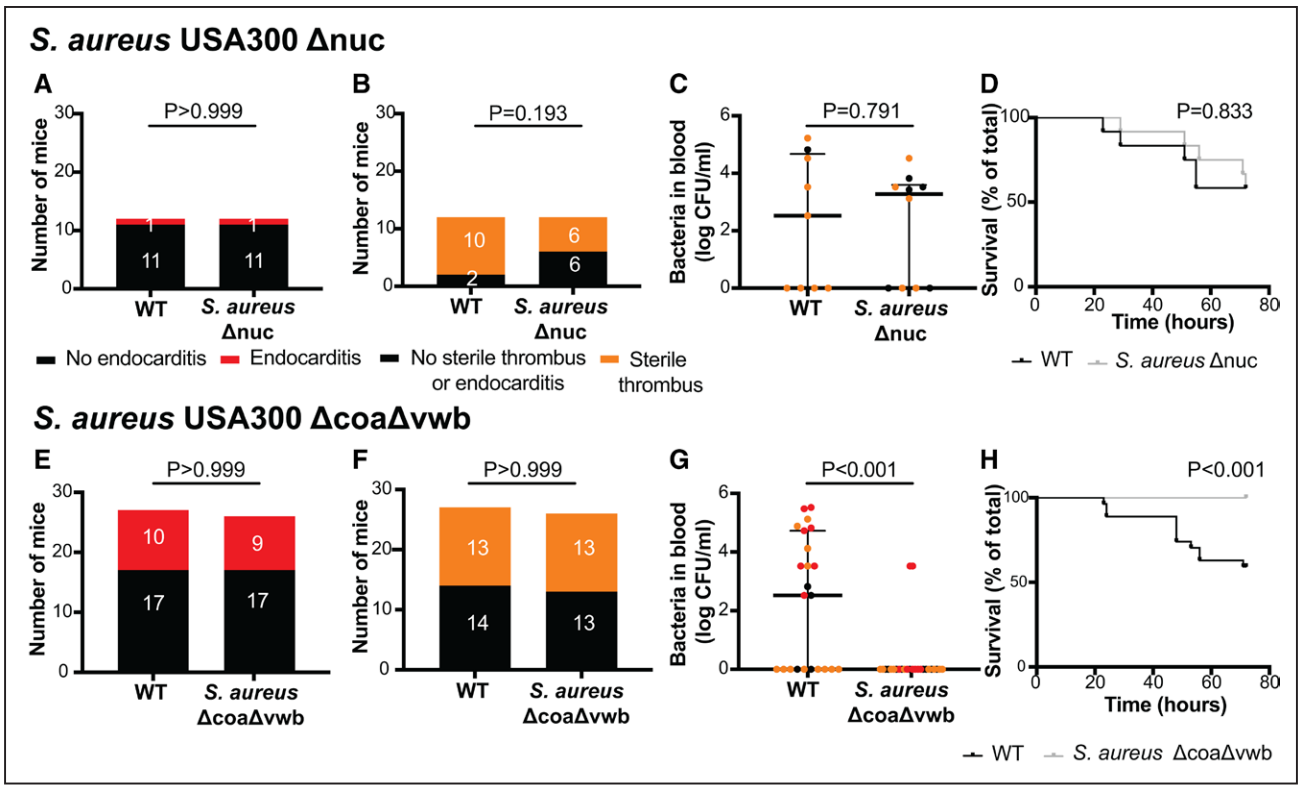

Figure 7. Absence of staphylocoagulases, but not of nucleases, improves endocarditis outcome.
A–**D**, Proportions of mice that developed inflammation-induced endocarditis (**A**) or sterile thrombi (**B**) at day 3, bacteremia levels at end point (n=9, 10, **C**), and survival rates (n=12, 12, **D**) of mice infected with the nuclease mutant (Δnuc [nucleases]) compared to wild-type (WT) *Staphylococcus aureus* USA300. **E**–**H**, Proportions of mice that developed inflammation-induced endocarditis (**E**) or sterile thrombi (**F**) at day 3, bacteremia levels at endpoint (n=23, 26, **G**), and survival rates (n=27, 26, **H**) of mice infected with a mutant doubly deficient in ΔcoaΔvwb (coagulase and von Willebrand factor binding protein) compared to WT *S. aureus* USA300. Median (interquartile range) are represented in C and G. Fisher Exact (**A** and **B, E** and **F**), Mann-Whitney test (**C** and **G**), and log-rank (Mantel-Cox; **D** and **H**) tests were conducted to determine significance. CFU indicates colony-forming units.

species-dependent mechanisms.[41] However, we observed that *S. aureus*–induced NET formation was significantly reduced in neutrophil-selective PAD4 knockout mice both in vivo and in an in vitro assay, highlighting the importance of PAD4 in *S. aureus*–induced NET release. Recent evidence suggests a role of PAD4-mediated pathways in *S. aureus* toxin (PVL [Panton-Valentin leukocidin])-induced NET formation[44] and in MRSA sepsis.[49,50]

Large MPO- and H3Cit-positive infiltrates were typically detected in the surrounding vasculature, whereas in the direct vicinity of bacteria, their presence was rather limited. When NETs encounter *S. aureus*, their extracellular DNA backbone can be degraded by secreted nucleases. Infecting mice with *S. aureus* deficient in nuclease (Δnuc) did not alter endocarditis development and other outcomes, implying that NET degradation by *S. aureus* does not influence endocarditis progression in this model. Dense leukocyte infiltrates were also still detected in the aortic walls of mice infected with *S. aureus* Δnuc. Although these massive infiltrates have already been described in damage-induced IE by Gram and H&E staining or staining for myeloid markers and NE,[11,26,29,51,52] this study has now characterized these infiltrates as H3Cit, MPO, and Ly6G-positive.

We show that these massive infiltrates in IE vegetations, induced by different strains of *S. aureus*, coincided with extensive tissue destruction as evidenced by large areas of apoptotic cells. These TUNEL-positive areas also positively correlated with H3Cit, MPO, Ly6G, and bacteria located outside the infected vegetation. Our data implies that when our immune system fails to clear bacteria, damage to the surrounding tissue may be the result of both excessive immune response caused by neutrophils undergoing NETosis and proliferation of bacteria. Signs of proteolytic tissue damage and apoptosis have been shown to be present in vegetations of rats and patients, mainly caused by *Enterococcus faecalis* and *Streptococci*, and have been linked to host proteases, such as NE and plasmin.[12,26] Besides these markers, other neutrophils, NET components, and bacterial factors are likely to play prominent roles in tissue destruction. A proteomic analysis of endocarditis vegetations showed extensive proteolysis within vegetations and that 68% of the detected proteases could be attributed to proteases of host origin and 32% to pathogen-specific proteases.[53] *S. aureus*, in particular, can cause tissue damage and apoptosis via various proteases and toxins.[54,55] Furthermore, the degree of endothelial cell damage caused

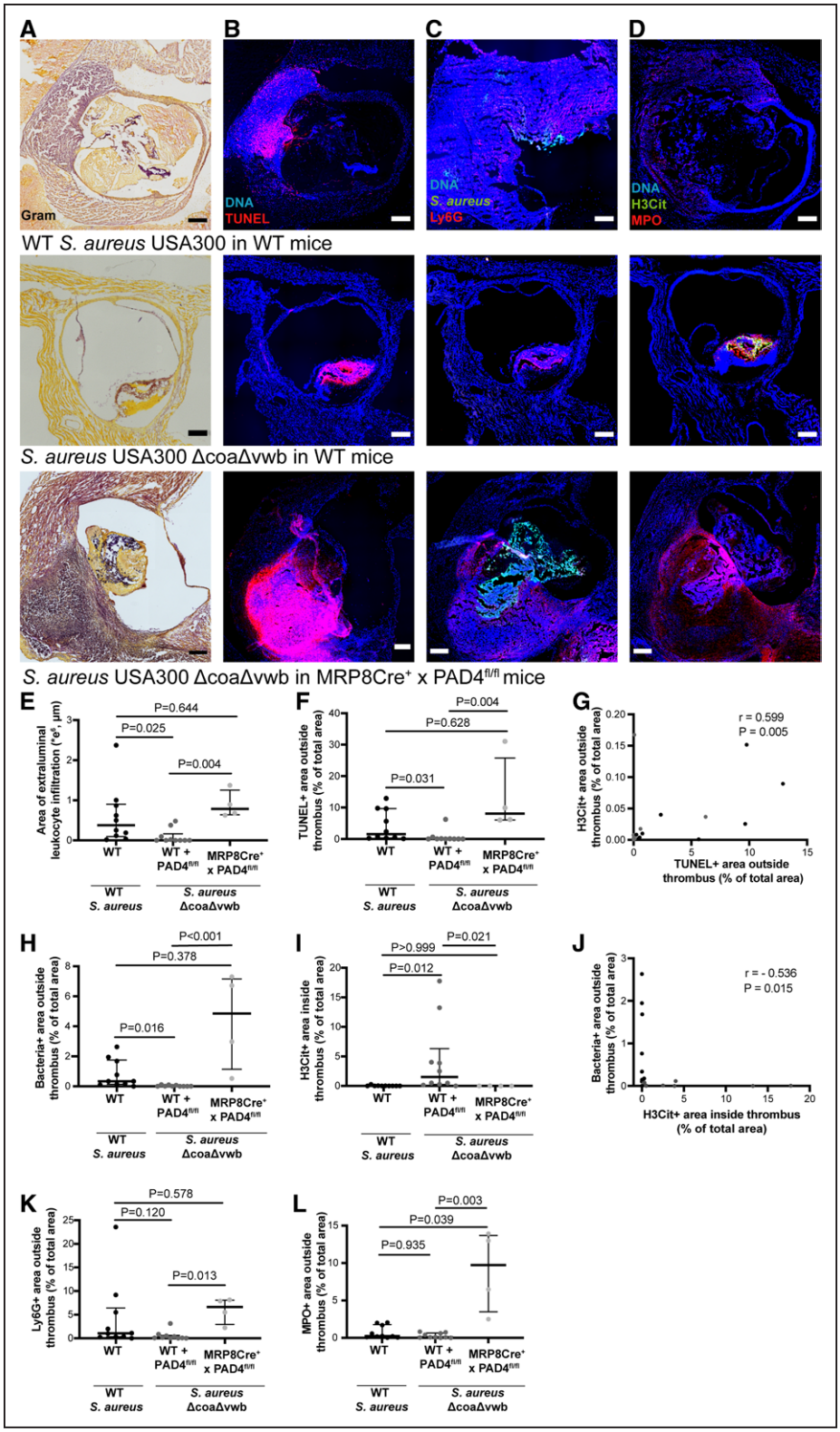

Figure 8. Staphylocoagulases prevent NETs (neutrophil extracellular traps) from constraining bacterial infection and promoting tissue destruction.

A, Brightfield images of a Brown-Hopps Gram stain (n=10, 10, 4) with bacteria represented in purple. **B**, Click-iT Plus TUNEL (terminal deoxynucleotidyl transferase dUTP nick-end labeling) assay stained images (n=10,10, 4), depicting apoptotic cells in red. **C** and **D**, Fluorescence microscopy images (n=10, 10, 4) of *Staphylococcus aureus* in green and neutrophil-specific marker Ly6G in red (**C**), and MPO (myeloperoxidase) in red and H3Cit (citrullinated histone H3) in green (**D**). DNA is stained with Hoechst 33342 in blue. Scale bars represent 200 µm. **E**–**L**, Quantifications of extraluminal leukocyte infiltration (**E**), TUNEL (**F**), bacteria (**H**), Ly6G (**K**), and MPO (**L**)-positive area situated outside infected thrombi and (*Continued*)

Figure 8 Continued. H3Cit inside the thrombus (**I**) in control (C57Bl/6J) mice with infective endocarditis induced by wild-type (WT; black, n=10) *S. aureus*, and in control (C57Bl/6J and PAD4 (peptidylarginine deiminase 4)$^{fl/fl}$, dark gray, n=10) and neutrophil-selective PAD4 knockout mice (MRP8Cre^{+}×PAD4$^{fl/fl}$, light gray, n=4) with infective endocarditis induced by *S. aureus* coaΔvwb (coagulase and von Willebrand factor binding protein). **G**, Spearman correlation between the H3Cit-positive area and TUNEL-positive area, both located outside the infected vegetations caused by WT (n=10, C57Bl/6J) and *S. aureus* ΔcoaΔvwb (n=10, C57Bl/6J and PAD4$^{fl/fl}$). **J**, Spearman correlation between bacteria located outside the vegetation and H3Cit inside the thrombus infected with WT (n=10, C57Bl/6J) and *S. aureus* ΔcoaΔvwb (n=10, C57Bl/6J and PAD4$^{fl/fl}$). Median (interquartile range) are represented in **E** and **F**, **H** and **I**, **K** and **L**. Significance was determined by Kruskal-Wallis test with Dunn post test (**E** and **F**, **H** and **I**, **K** and **L**). MRP8Cre+ indicates myeloid related protein 8, Cre recombinase expressing.

by clinical MRSA isolates in vitro has been shown to be positively correlated with their virulence in an IE rabbit model.[56] As there was no difference in the apoptosis-positive area between neutrophil-selective PAD4 knockout and control mice, NETs are not likely to be the sole cause for this destruction.

Despite extensive NET release in IE, outcomes were not altered in animals with impaired PAD4-mediated NETosis or when wild-type animals were challenged with *S. aureus* Δnuc. We hypothesized that neutrophils may be unable to reach bacteria inside the vegetation. Recent evidence showed that a staphylocoagulase-induced fibrin-layer shielded myeloid cells from entering IE vegetations in mice.[29,51] Histological examination of a late-stage human vegetation confirmed that the bacteria-rich core is typically surrounded by a bacteria-free region composed of fibrin and platelets.[57] Interestingly, preventing the formation of the protective fibrin-layer with antibodies against Coa and vWbp facilitated Ly6G+ neutrophil entry into a femoral artery vegetation.[29] Here, we report that infecting mice with *S. aureus* USA300 ΔcoaΔvwb prevented the accumulation of leukocyte infiltrates in the adjacent vasculature, more specifically the accumulation of Ly6G- and bacteria-positive infiltrates. Remarkably, the apoptosis typically induced by these infiltrates was essentially absent in mice with *S. aureus* ΔcoaΔvwb-induced vegetations. In addition to the beneficial effects on infiltration and apoptosis size, use of an *S. aureus* strain deficient in these staphylocoagulases improved overall outcome, as these mice displayed decreased mortality and bacteriemia levels. In line with our findings, genetic deletion and antibody-mediated therapy against both Coa and vWbp improved survival in animal models of damage-induced IE, sepsis, and abscess formation.[29,36,51,58]

Besides physically shielding neutrophils from the bacteria-rich thrombus, the staphylothrombin-mediated fibrin shield has been shown to inhibit leukocyte activation, phagocytosis, and phagocytotic killing.[59,60] A link between staphylocoagulases and NETs, however, had not been explored yet. Our study provides new evidence for the involvement of NETs in the beneficial effects of preventing staphylocoagulase-induced fibrin. In the presence of such a physical barrier, neutrophils may not be able to reach their target and carry out their bactericidal function via NET release. Remarkably, vegetations induced by *S. aureus* ΔcoaΔvwb contained excessive amounts of NETs, and the NET-specific marker H3Cit located inside the vegetation negatively correlated with bacteria and apoptosis outside this vegetation. This reveals that staphylocoagulases prevent future NET-releasing neutrophils from entering the thrombus and constraining bacterial replication and tissue destruction. Furthermore, we showed that these beneficial effects on bacteria replication and tissue destruction in the adjacent vasculature were abolished when mice with impaired NET formation were infected with *S. aureus* ΔcoaΔvwb. Additionally, these findings could explain why impairment of NET formation by neutrophil-selective PAD4 knockout mice was ineffective in preventing endocarditis. Although injecting mice with *S. aureus* ΔcoaΔvwb clearly improved outcome, the proportion of mice that developed endocarditis was not altered, which has also been reported by others.[29,61] Some groups have stated that the extracellular DNA fibers from NETs form a scaffold that constrains but does not kill *S. aureus*.[23,42,43,62,63] In that case, antibiotics would likely be needed to kill the bacteria inside the vegetation. Combining dabigatran with gentamycin has been shown to effectively reduce vegetation size and the bacterial load on aortic valves of rats with IE.[64]

In conclusion, we show that neutrophils and NETs are abundantly present in mice with inflammation-induced IE and that neutrophils protect against IE independent of PAD4-mediated NET release. The ability of *S. aureus* to drive fibrin formation likely shields neutrophils from entering the thrombus. In absence of staphylocoagulases, NETs are able to constrain the infection and thus hamper tissue damage. This work uncovers a potential new evasion strategy against an innate host defense mechanism whereby the bactericidal activity of NETs is negated by *S. aureus* coagulases.

ARTICLE INFORMATION

Received April 15, 2022; accepted November 22, 2022.

Affiliations

Center for Molecular and Vascular Biology, Department of Cardiovascular Sciences (S.M., M.L., S.K., L.L., C.P.M., L.F., S.V.B., T.V., P.V., K.M.) and Electron Microscopy-Platform of the VIB Bio Imaging Core and VIB Center for Brain and Disease Research (P.B.), KU Leuven, Belgium. Department of Life Sciences, Manchester Metropolitan University, United Kingdom (M.C.). Department of Microbiology, University of Chicago, IL (D.M.).

Acknowledgments

We thank the UZ Leuven staff for the collection of the clinical staphylococcal strains.

Sources of Funding

S. Meyers and C. Martens are fellows of the Fonds Wetenschappelijk Onderzoek Vlaanderen (FWO; 1S77119N to S.M., 11B0621N to C.M.). D. Missiakas is supported by a National Institutes of Health, National Institute of Allergy and Infectious Diseases award (NIH NIAID AI052474). Our research on this subject is funded by FWO research grants 1514518N and 1525319N, KU Leuven Internal Fund Starting Grant number STG/18/048 to K. Martinod, FWO research project number G066021N to P. Verhamme and T. Vanassche, and KU Leuven Internal Fund grant number C24M/20/056 to P. Verhamme and T. Vanassche.

Disclosures

None.

Supplemental Material

Major Resources Table
ARRIVE Checklist
Supplemental Methods
Figures S1–S7
Tables S1 and S2

REFERENCES

1. Vogkou CT, Vlachogiannis NI, Palaiodimos L, Kousoulis AA. The causative agents in infective endocarditis: a systematic review comprising 33,214 cases. *Eur J Clin Microbiol Infect Dis*. 2016;35:1227–1245. doi: 10.1007/s10096-016-2660-6
2. Yang X, Chen H, Zhang D, Shen L, An G, Zhao S. Global magnitude and temporal trend of infective endocarditis, 1990-2019: results from the global burden of disease study. *Eur J Prev Cardiol*. 2021;29:1227. doi: 10.1093/eurjpc/zwab184
3. Talha KM, Baddour LM, Thornhill MH, Arshad V, Tariq W, Tleyjeh IM, Scott CG, Hyun MC, Bailey KR, Anavekar NS, et al. Escalating incidence of infective endocarditis in Europe in the 21st century. *Open Heart*. 2021;8:e001846. doi: 10.1136/openhrt-2021-001846
4. Dayer MJ, Jones S, Prendergast B, Baddour LM, Lockhart PB, Thornhill MH. Incidence of infective endocarditis in England, 2000-13: a secular trend, interrupted time-series analysis. *Lancet*. 2015;385:1219–1228. doi: 10.1016/S0140-6736(14)62007-9
5. Miro JM, Anguera I, Cabell CH, Chen AY, Stafford JA, Corey GR, Olaison L, Eykyn S, Hoen B, Abrutyn E, et al; International Collaboration on Endocarditis Merged Database Study Group. Staphylococcus aureus native valve infective endocarditis: report of 566 episodes from the International Collaboration on Endocarditis Merged Database. *Clin Infect Dis*. 2005;41:507–514. doi: 10.1086/431979
6. Nadji G, Remadi JP, Coviaux F, Mirode AA, Brahim A, Enriquez-Sarano M, Tribouilloy C. Comparison of clinical and morphological characteristics of Staphylococcus aureus endocarditis with endocarditis caused by other pathogens. *Heart*. 2005;91:932–937. doi: 10.1136/hrt.2004.042648
7. Hill EE, Herijgers P, Claus P, Vanderschueren S, Herregods MC, Peetermans WE. Infective endocarditis: changing epidemiology and predictors of 6-month mortality: a prospective cohort study. *Eur Heart J*. 2007;28:196–203. doi: 10.1093/eurheartj/ehl427
8. Habib G, Erba PA, Iung B, Donal E, Cosyns B, Laroche C, Popescu BA, , Prendergast B, Tornos P, et al; EURO-ENDO Investigators. Clinical presentation, aetiology and outcome of infective endocarditis. Results of the ESC-EORP EURO-ENDO (European infective endocarditis) registry: a prospective cohort study. *Eur Heart J*. 2019;40:3222–3232. doi: 10.1093/eurheartj/ehz620
9. Rosenbach O. Ueberartificiele Herzklappenfehler, Eine experimentellpathologische Abhandlung. *Arch Exp Pathol Pharmak*. 1878;9:1–30.
10. Garrison PK, Freedman LR. Experimental endocarditis I. Staphylococcal endocarditis in rabbits resulting from placement of a polyethylene catheter in the right side of the heart. *Yale J Biol Med*. 1970; 42: 394–410.
11. Gibson GW, Kreuser SC, Riley JM, Rosebury-Smith WS, Courtney CL, Juneau PL, Hollembaek JM, Zhu T, Huband MD, Brammer DW, et al. Development of a mouse model of induced Staphylococcus aureus infective endocarditis. *Comp Med*. 2007;57:563–569.
12. Augustin P, Alsalih G, Launey Y, Delbosc S, Louedec L, Ollivier V, Chau F, Montravers P, Duval X, Michel JB, et al. Predominant role of host proteases in myocardial damage associated with infectious endocarditis induced by Enterococcus faecalis in a rat model. *Infect Immun*. 2013;81:1721–1729. doi: 10.1128/IAI.00775-12
13. Jung CJ, Yeh CY, Hsu RB, Lee CM, Shun CT, Chia JS. Endocarditis pathogen promotes vegetation formation by inducing intravascular neutrophil extracellular traps through activated platelets. *Circulation*. 2015;131:571–581. doi: 10.1161/CIRCULATIONAHA.114.011432
14. Hsu CC, Hsu RB, Ohniwa RL, Chen JW, Yuan CT, Chia JS, Jung CJ. Neutrophil extracellular traps enhance staphylococcus aureus vegetation formation through interaction with platelets in infective endocarditis. *Thromb Haemost*. 2019;119:786–796. doi: 10.1055/s-0039-1678665
15. Schwarz C, Tore Y, Hoesker V, Ameling S, Grun K, Volker U, Schulze PC, Franz M, Faber C, Schaumburg F, et al. Host-pathogen interactions of clinical S. aureus isolates to induce infective endocarditis. *Virulence*. 2021;12:2073–2087. doi: 10.1080/21505594.2021.1960107
16. Selton-Suty C, Celard M, Le Moing V, Doco-Lecompte T, Chirouze C, Iung B, Strady C, Revest M, Vandenesch F, Bouvet A, et al.; AEPEI Study Group. Preeminence of Staphylococcus aureus in infective endocarditis: a 1-year population-based survey. *Clin Infect Dis*. 2012;54:1230–1239. doi: 10.1093/cid/cis199
17. Le Moing V, Alla F, Doco-Lecompte T, Delahaye F, Piroth L, Chirouze C, Tattevin P, Lavigne JP, Erpelding ML, Hoen B, et al. Staphylococcus aureus bloodstream infection and endocarditis--a prospective cohort study. *PLoS One*. 2015;10:e0127385. doi: 10.1371/journal.pone.0127385
18. Olmos C, Vilacosta I, Fernandez C, Sarria C, Lopez J, Del Trigo M, Ferrera C, Vivas D, Maroto L, Hernandez M, et al. Comparison of clinical features of left-sided infective endocarditis involving previously normal versus previously abnormal valves. *Am J Cardiol*. 2014;114:278–283. doi: 10.1016/j.amjcard.2014.04.036
19. Sun BJ, Choi SW, Park KH, Jang JY, Kim DH, Song JM, Kang DH, Kim YS, Song JK. Infective endocarditis involving apparently structurally normal valves in patients without previously recognized predisposing heart disease. *J Am Coll Cardiol*. 2015;65:307–309. doi: 10.1016/j.jacc.2014.10.046
20. Liesenborghs L, Meyers S, Lox M, Criel M, Claes J, Peetermans M, Trenson S, Vande Velde G, Vanden Berghe P, Baatsen P, et al. Staphylococcus aureus endocarditis: distinct mechanisms of bacterial adhesion to damaged and inflamed heart valves. *Eur Heart J*. 2019;40:3248–3259. doi: 10.1093/eurheartj/ehz175
21. Martinod K, Deppermann C. Immunothrombosis and thromboinflammation in host defense and disease. *Platelets*. 2021;32:314–324. doi: 10.1080/09537104.2020.1817360
22. Brinkmann V, Reichard U, Goosmann C, Fauler B, Uhlemann Y, Weiss DS, Weinrauch Y, Zychlinsky A. Neutrophil extracellular traps kill bacteria. *Science*. 2004;303:1532–1535. doi: 10.1126/science.1092385
23. McDonald B, Urrutia R, Yipp BG, Jenne CN, Kubes P. Intravascular neutrophil extracellular traps capture bacteria from the bloodstream during sepsis. *Cell Host Microbe*. 2012;12:324–333. doi: 10.1016/j.chom.2012.06.011
24. Fuchs TA, Brill A, Duerschmied D, Schatzberg D, Monestier M, Myers DD Jr, Wrobleski SK, Wakefield TW, Hartwig JH, Wagner DD. Extracellular DNA traps promote thrombosis. *Proc Natl Acad Sci USA*. 2010;107:15880–15885. doi: 10.1073/pnas.1005743107
25. Meyers S, Crescente M, Verhamme P, Martinod K. Staphylococcus aureus and Neutrophil Extracellular traps: the master manipulator meets its match in immunothrombosis. *Arterioscler Thromb Vasc Biol*. 2022;42:261–276. doi: 10.1161/ATVBAHA.121.316930
26. Al-Salih G, Al-Attar N, Delbosc S, Louedec L, Corvazier E, Loyau S, Michel JB, Pidard D, Duval X, Meilhac O. Role of vegetation-associated protease activity in valve destruction in human infective endocarditis. *PLoS One*. 2012;7:e45695. doi: 10.1371/journal.pone.0045695
27. Thammavongsa V, Kim HK, Missiakas D, Schneewind O. Staphylococcal manipulation of host immune responses. *Nat Rev Microbiol*. 2015;13:529–543. doi: 10.1038/nrmicro3521
28. Liesenborghs L, Verhamme P, Vanassche T. Staphylococcus aureus, master manipulator of the human hemostatic system. *J Thromb Haemost*. 2018;16:441–454. doi: 10.1111/jth.13928
29. Panizzi P, Krohn-Grimberghe M, Keliher E, et al. Multimodal imaging of bacterial-host interface in mice and piglets with Staphylococcus aureus endocarditis. *Sci Transl Med*. 2020;12:eaay2104. doi: 10.1126/scitranslmed.aay2104
30. Bjornsdottir H, Dahlstrand Rudin A, Klose FP, Elmwall J, Welin A, Stylianou M, Christenson K, Urban CF, Forsman H, Dahlgren C, et al. Phenol-soluble modulin alpha peptide toxins from aggressive staphylococcus aureus induce rapid formation of neutrophil extracellular traps through a reactive oxygen species-independent pathway. *Front Immunol*. 2017;8:257. doi: 10.3389/fimmu.2017.00257
31. Berends ET, Horswill AR, Haste NM, Monestier M, Nizet V, von Kockritz-Blickwede M. Nuclease expression by Staphylococcus aureus facilitates escape from neutrophil extracellular traps. *J Innate Immun*. 2010;2:576–586. doi: 10.1159/000319909

32. Li P, Li M, Lindberg MR, Kennett MJ, Xiong N, Wang Y. PAD4 is essential for antibacterial innate immunity mediated by neutrophil extracellular traps. *J Exp Med*. 2010;207:1853–1862. doi: 10.1084/jem.20100239
33. Martinod K, Demers M, Fuchs TA, Wong SL, Brill A, Gallant M, Hu J, Wang Y, Wagner DD. Neutrophil histone modification by peptidylarginine deiminase 4 is critical for deep vein thrombosis in mice. *Proc Natl Acad Sci USA*. 2013;110:8674–8679. doi: 10.1073/pnas.1301059110
34. Thiam HR, Wong SL, Qiu R, Kittisopikul M, Vahabikashi A, Goldman AE, Goldman RD, Wagner DD, Waterman CM. NETosis proceeds by cytoskeleton and endomembrane disassembly and PAD4-mediated chromatin decondensation and nuclear envelope rupture. *Proc Natl Acad Sci USA*. 2020;117:7326–7337. doi: 10.1073/pnas.1909546117
35. Thammavongsa V, Missiakas DM, Schneewind O. Staphylococcus aureus degrades neutrophil extracellular traps to promote immune cell death. *Science*. 2013;342:863–866. doi: 10.1126/science.1242255
36. Cheng AG, McAdow M, Kim HK, Bae T, Missiakas DM, Schneewind O. Contribution of coagulases towards Staphylococcus aureus disease and protective immunity. *PLoS Pathog*. 2010;6:e1001036. doi: 10.1371/journal.ppat.1001036
37. Boivin G, Faget J, Ancey PB, Gkasti A, Mussard J, Engblom C, Pfirschke C, Contat C, Pascual J, Vazquez J, et al. Durable and controlled depletion of neutrophils in mice. *Nat Commun*. 2020;11:2762. doi: 10.1038/s41467-020-16596-9
38. Demers M, Krause DS, Schatzberg D, Martinod K, Voorhees JR, Fuchs TA, Scadden DT, Wagner DD. Cancers predispose neutrophils to release extracellular DNA traps that contribute to cancer-associated thrombosis. *Proc Natl Acad Sci USA*. 2012;109:13076–13081. doi: 10.1073/pnas.1200419109
39. Bitschar K, Staudenmaier L, Klink L, Focken J, Sauer B, Fehrenbacher B, Herster F, Bittner Z, Bleul L, Schaller M, et al. Staphylococcus aureus skin colonization is enhanced by the interaction of neutrophil extracellular traps with keratinocytes. *J Invest Dermatol*. 2020;140:1054–1065.e4. doi: 10.1016/j.jid.2019.10.017
40. Hoppenbrouwers T, Autar ASA, Sultan AR, Abraham TE, van Cappellen WA, Houtsmuller AB, van Wamel WJB, van Beusekom HMM, van Neck JW, de Maat MPM. In vitro induction of NETosis: comprehensive live imaging comparison and systematic review. *PLoS One*. 2017;12:e0176472. doi: 10.1371/journal.pone.0176472
41. Pilszek FH, Salina D, Poon KK, Fahey C, Yipp BG, Sibley CD, Robbins SM, Green FH, Surette MG, Sugai M, et al. A novel mechanism of rapid nuclear neutrophil extracellular trap formation in response to Staphylococcus aureus. *J Immunol*. 2010;185:7413–7425. doi: 10.4049/jimmunol.1000675
42. Bhattacharya M, Berends ETM, Chan R, Schwab E, Roy S, Sen CK, Torres VJ, Wozniak DJ. Staphylococcus aureus biofilms release leukocidins to elicit extracellular trap formation and evade neutrophil-mediated killing. *Proc Natl Acad Sci USA*. 2018;115:7416–7421. doi: 10.1073/pnas.1721949115
43. Malachowa N, Kobayashi SD, Freedman B, Dorward DW, DeLeo FR. Staphylococcus aureus leukotoxin GH promotes formation of neutrophil extracellular traps. *J Immunol*. 2013;191:6022–6029. doi: 10.4049/jimmunol.1301821
44. Mazzoleni V, Zimmermann K, Smirnova A, Tarassov I, Prevost G. Staphylococcus aureus Panton-Valentine Leukocidin triggers an alternative NETosis process targeting mitochondria. *FASEB J*. 2021;35:e21167. doi: 10.1096/fj.201902981R
45. Cogen AL, Yamasaki K, Muto J, Sanchez KM, Crotty Alexander L, Tanios J, Lai Y, Kim JE, Nizet V, Gallo RL. Staphylococcus epidermidis antimicrobial delta-toxin (phenol-soluble modulin-gamma) cooperates with host antimicrobial peptides to kill group A Streptococcus. *PLoS One*. 2010;5:e8557. doi: 10.1371/journal.pone.0008557
46. Staudenmaier L, Focken J, Schlatterer K, Kretschmer D, Schittek B. Bacterial membrane vesicles shape Staphylococcus aureus skin colonization and induction of innate immune responses. *Exp Dermatol*. 2022;31:349–361. doi: 10.1111/exd.14478
47. Dengler V, Foulston L, DeFrancesco AS, Losick R. An electrostatic net model for the role of extracellular DNA in biofilm formation by Staphylococcus aureus. *J Bacteriol*. 2015;197:3779–3787. doi: 10.1128/JB.00726-15
48. Sultan AR, Hoppenbrouwers T, Lemmens-den Toom NA, Snijders SV, van Neck JW, Verbon A, de Maat MPM, van Wamel WJB. During the early stages of Staphylococcus aureus biofilm formation, induced neutrophil extracellular traps are degraded by autologous thermonuclease. *Infect Immun*. 2019;87:e6005. . doi: 10.1128/IAI.00605-19
49. Kolaczkowska E, Jenne CN, Surewaard BG, Thanabalasuriar A, Lee WY, Sanz MJ, Mowen K, Opdenakker G, Kubes P. Molecular mechanisms of NET formation and degradation revealed by intravital imaging in the liver vasculature. *Nat Commun*. 2015;6:6673. doi: 10.1038/ncomms7673
50. McDonald B, Davis RP, Kim SJ, Tse M, Esmon CT, Kolaczkowska E, Jenne CN. Platelets and neutrophil extracellular traps collaborate to promote intravascular coagulation during sepsis in mice. *Blood*. 2017;129:1357–1367. doi: 10.1182/blood-2016-09-741298
51. Panizzi P, Nahrendorf M, Figueiredo JL, Panizzi J, Marinelli B, Iwamoto Y, Keliher E, Maddur AA, Waterman P, et al. In vivo detection of Staphylococcus aureus endocarditis by targeting pathogen-specific prothrombin activation. *Nat Med*. 2011;17:1142–1146. doi: 10.1038/nm.2423
52. Schwarz C, Hoerr V, Tore Y, Hosker V, Hansen U, Van de Vyver H, Niemann S, Kuhlmann MT, Jeibmann A, Wildgruber M, et al. Isolating crucial steps in induction of infective endocarditis with preclinical modeling of host pathogen interaction. *Front Microbiol*. 2020;11:1325. doi: 10.3389/fmicb.2020.01325
53. Martin DR, Witten JC, Tan CD, Rodriguez ER, Blackstone EH, Pettersson GB, Seifert DE, Willard BB, Apte SS. Proteomics identifies a convergent innate response to infective endocarditis and extensive proteolysis in vegetation components. *JCI Insight*. 2020;5:e135317. doi: 10.1172/jci.insight.135317
54. Pietrocola G, Nobile G, Rindi S, Speziale P. Staphylococcus aureus manipulates innate immunity through own and host-expressed proteases. *Front Cell Infect Microbiol*. 2017;7:166. doi: 10.3389/fcimb.2017.00166
55. Zhang X, Hu X, Rao X. Apoptosis induced by Staphylococcus aureus toxins. *Microbiol Res*. 2017;205:19–24. doi: 10.1016/j.micres.2017.08.006
56. Seidl K, Bayer AS, McKinnell JA, Ellison S, Filler SG, Xiong YQ. In vitro endothelial cell damage is positively correlated with enhanced virulence and poor vancomycin responsiveness in experimental endocarditis due to methicillin-resistant Staphylococcus aureus. *Cell Microbiol*. 2011;13:1530–1541. doi: 10.1111/j.1462-5822.2011.01639.x
57. Baudoin JP, Camoin-Jau L, Prasanth A, Habib G, Lepidi H, Hannachi N. Ultrastructure of a late-stage bacterial endocarditis valve vegetation. *J Thromb Thrombol*. 2021;51:821–826. doi: 10.1007/s11239-020-02232-2
58. McAdow M, Kim HK, Dedent AC, Hendrickx AP, Schneewind O, Missiakas DM. Preventing Staphylococcus aureus sepsis through the inhibition of its agglutination in blood. *PLoS Pathog*. 2011;7:e1002307. doi: 10.1371/journal.ppat.1002307
59. Vanassche T, Verhaegen J, Peetermans WE, Ryan JVAN, Cheng A, Schneewind O, Hoylaerts MF, Verhamme P. Inhibition of staphylothrombin by dabigatran reduces Staphylococcus aureus virulence. *J Thromb Haemost*. 2011;9:2436–2446. doi: 10.1111/j.1538-7836.2011.04529.x
60. Thomer L, Emolo C, Thammavongsa V, Kim HK, McAdow ME, Yu W, Kieffer M, Schneewind O, Missiakas D. Antibodies against a secreted product of Staphylococcus aureus trigger phagocytic killing. *J Exp Med*. 2016;213:293–301. doi: 10.1084/jem.20150074
61. Mancini S, Oechslin F, Menzi C, Que YA, Claes J, Heying R, Veloso TR, Vanassche T, Missiakas D, Schneewind O, et al. Marginal role of von Willebrand factor-binding protein and coagulase in the initiation of endocarditis in rats with catheter-induced aortic vegetations. *Virulence*. 2018;9:1615–1624. doi: 10.1080/21505594.2018.1528845
62. Azzouz L, Cherry A, Riedl M, Khan M, Pluthero FG, Kahr WHA, Palaniyar N, Licht C. Relative antibacterial functions of complement and NETs: NETs trap and complement effectively kills bacteria. *Mol Immunol*. 2018;97:71–81. doi: 10.1016/j.molimm.2018.02.019
63. Menegazzi R, Decleva E, Dri P. Killing by neutrophil extracellular traps: fact or folklore?. *Blood*. 2012;119:1214–1216. doi: 10.1182/blood-2011-07-364604
64. Lerche CJ, Christophersen LJ, Goetze JP, Nielsen PR, Thomsen K, Enevold C, Hoiby N, Jensen PO, Bundgaard H, Moser C. Adjunctive dabigatran therapy improves outcome of experimental left-sided Staphylococcus aureus endocarditis. *PLoS One*. 2019;14:e0215333. doi: 10.1371/journal.pone.0215333